

---

# **NONLINEAR DYNAMICS AND CHAOS**

*With Applications to  
Physics, Biology, Chemistry,  
and Engineering*

---

**Steven H. Strogatz**



**CRC Press**

Taylor & Francis Group

Boca Raton London New York

---

CRC Press is an imprint of the  
Taylor & Francis Group, an **informa** business  
A CHAPMAN & HALL BOOK

# 10

---

## ONE-DIMENSIONAL MAPS

---

### 10.0 Introduction

This chapter deals with a new class of dynamical systems in which time is *discrete*, rather than continuous. These systems are known variously as difference equations, recursion relations, iterated maps, or simply *maps*.

For instance, suppose you repeatedly press the cosine button on your calculator, starting from some number  $x_0$ . Then the successive readouts are  $x_1 = \cos x_0$ ,  $x_2 = \cos x_1$ , and so on. Set your calculator to radian mode and try it. Can you explain the surprising result that emerges after many iterations?

The rule  $x_{n+1} = \cos x_n$  is an example of a *one-dimensional map*, so-called because the points  $x_n$  belong to the one-dimensional space of real numbers. The sequence  $x_0, x_1, x_2, \dots$  is called the *orbit* starting from  $x_0$ .

Maps arise in various ways:

1. *As tools for analyzing differential equations.* We have already encountered maps in this role. For instance, Poincaré maps allowed us to prove the existence of a periodic solution for the driven pendulum and Josephson junction (Section 8.5), and to analyze the stability of periodic solutions in general (Section 8.7). The Lorenz map (Section 9.4) provided strong evidence that the Lorenz attractor is truly strange, and is not just a long-period limit cycle.
2. *As models of natural phenomena.* In some scientific contexts it is natural to regard time as discrete. This is the case in digital electronics, in parts of economics and finance theory, in impulsively driven mechanical systems, and in the study of certain animal populations where successive generations do not overlap.
3. *As simple examples of chaos.* Maps are interesting to study in their own right, as mathematical laboratories for chaos. Indeed, maps are capable

of much wilder behavior than differential equations because the points  $x_n$  *hop* along their orbits rather than flow continuously (Figure 10.0.1).



**Figure 10.0.1**

The study of maps is still in its infancy, but exciting progress has been made in the last few decades, thanks to the growing availability of calculators, then computers, and now computer graphics. Maps are easy and fast to simulate on digital computers where time is *inherently* discrete. Such computer experiments have revealed a number of unexpected and beautiful patterns, which in turn have stimulated new theoretical developments. Most surprisingly, maps have generated a number of successful predictions about the routes to chaos in semiconductors, convecting fluids, heart cells, lasers, and chemical oscillators.

We discuss some of the properties of maps and the techniques for analyzing them in Sections 10.1–10.5. The emphasis is on period-doubling and chaos in the logistic map. Section 10.6 introduces the amazing idea of universality, and summarizes experimental tests of the theory. Section 10.7 is an attempt to convey the basic ideas of Feigenbaum’s renormalization technique.

As usual, our approach will be intuitive. For rigorous treatments of one-dimensional maps, see Devaney (1989) and Collet and Eckmann (1980).

## 10.1 Fixed Points and Cobwebs

In this section we develop some tools for analyzing one-dimensional maps of the form  $x_{n+1} = f(x_n)$ , where  $f$  is a smooth function from the real line to itself.

### A Pedantic Point

When we say “map,” do we mean the function  $f$  or the difference equation  $x_{n+1} = f(x_n)$ ? Following common usage, we’ll call *both* of them maps. If you’re disturbed by this, you must be a pure mathematician . . . or should consider becoming one!

### Fixed Points and Linear Stability

Suppose  $x^*$  satisfies  $f(x^*) = x^*$ . Then  $x^*$  is a **fixed point**, for if  $x_n = x^*$  then  $x_{n+1} = f(x_n) = f(x^*) = x^*$ ; hence the orbit remains at  $x^*$  for all future iterations.

To determine the stability of  $x^*$ , we consider a nearby orbit  $x_n = x^* + \eta_n$  and ask whether the orbit is attracted to or repelled from  $x^*$ . That is, does the deviation  $\eta_n$  grow or decay as  $n$  increases? Substitution yields

$$x^* + \eta_{n+1} = x_{n+1} = f(x^* + \eta_n) = f(x^*) + f'(x^*)\eta_n + O(\eta_n^2).$$

But since  $f(x^*) = x^*$ , this equation reduces to

$$\eta_{n+1} = f'(x^*)\eta_n + O(\eta_n^2).$$

Suppose we can safely neglect the  $O(\eta_n^2)$  terms. Then we obtain the *linearized map*  $\eta_{n+1} = f'(x^*)\eta_n$  with *eigenvalue* or **multiplier**  $\lambda = f'(x^*)$ . The solution of this linear map can be found explicitly by writing a few terms:  $\eta_1 = \lambda\eta_0$ ,  $\eta_2 = \lambda\eta_1 = \lambda^2\eta_0$ , and so in general  $\eta_n = \lambda^n\eta_0$ . If  $|\lambda| = |f'(x^*)| < 1$ , then  $\eta_n \rightarrow 0$  as  $n \rightarrow \infty$  and the fixed point  $x^*$  is **linearly stable**. Conversely, if  $|f'(x^*)| > 1$  the fixed point is **unstable**. Although these conclusions about local stability are based on linearization, they can be proven to hold for the original nonlinear map. But the linearization tells us nothing about the **marginal** case  $|f'(x^*)| = 1$ ; then the neglected  $O(\eta_n^2)$  terms determine the local stability. (All of these results have parallels for differential equations—recall Section 2.4.)

---

### EXAMPLE 10.1.1:

Find the fixed points for the map  $x_{n+1} = x_n^2$  and determine their stability.

*Solution:* The fixed points satisfy  $x^* = (x^*)^2$ . Hence  $x^* = 0$  or  $x^* = 1$ . The multiplier is  $\lambda = f'(x^*) = 2x^*$ . The fixed point  $x^* = 0$  is stable since  $|\lambda| = 0 < 1$ , and  $x^* = 1$  is unstable since  $|\lambda| = 2 > 1$ . ■

Try Example 10.1.1 on a hand calculator by pressing the  $x^2$  button over and over. You'll see that for sufficiently small  $x_0$ , the convergence to  $x^* = 0$  is *extremely* rapid. Fixed points with multiplier  $\lambda = 0$  are called **superstable** because perturbations decay like  $\eta_n \sim \eta_0^{(2^n)}$ , which is much faster than the usual  $\eta_n \sim \lambda^n\eta_0$  at an ordinary stable point.

### Cobwebs

In Section 8.7 we introduced the **cobweb** construction for iterating a map (Figure 10.1.1).

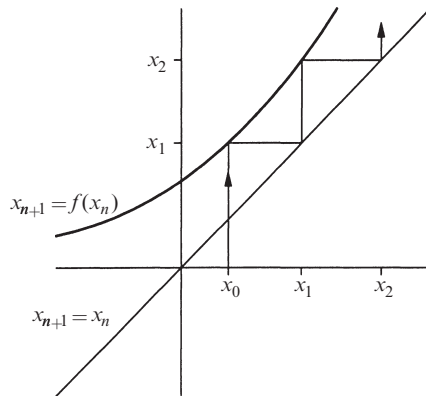


**Figure 10.1.1**

Given  $x_{n+1} = f(x_n)$  and an initial condition  $x_0$ , draw a vertical line until it intersects the graph of  $f$ ; that height is the output  $x_1$ . At this stage we could return to the horizontal axis and repeat the procedure to get  $x_2$  from  $x_1$ , but it is more convenient simply to trace a horizontal line till it intersects the diagonal line  $x_{n+1} = x_n$ , and then move vertically to the curve again. Repeat the process  $n$  times to generate the first  $n$  points in the orbit.

Cobwebs are useful because they allow us to see global behavior at a glance, thereby supplementing the local information available from the linearization. Cobwebs become even more valuable when linear analysis fails, as in the next example.

### **EXAMPLE 10.1.2:**

Consider the map  $x_{n+1} = \sin x_n$ . Show that the stability of the fixed point  $x^* = 0$  is not determined by the linearization. Then use a cobweb to show that  $x^* = 0$  is stable—in fact, *globally* stable.

*Solution:* The multiplier at  $x^* = 0$  is  $f'(0) = \cos(0) = 1$ , which is a marginal case where linear analysis is inconclusive. However, the cobweb of Figure 10.1.2 shows that  $x^* = 0$  is locally stable; the orbit slowly rattles down the narrow channel, and heads monotonically for the fixed point. (A similar picture is obtained for  $x_0 < 0$ .)

To see that the stability is global, we have to show that *all* orbits satisfy  $x_n \rightarrow 0$ . But for any  $x_0$ , the first iterate is sent immediately to the interval  $-1 \leq x_1 \leq 1$  since  $|\sin x| \leq 1$ . The cobweb in that interval looks qualitatively like Figure 10.1.2, so convergence is assured. ■

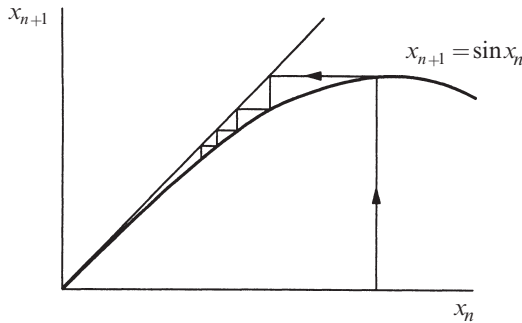


**Figure 10.1.2**

Finally, let's answer the riddle posed in Section 10.0.

### EXAMPLE 10.1.3:

Given  $x_{n+1} = \cos x_n$ , how does  $x_n$  behave as  $n \rightarrow \infty$ ?

*Solution:* If you tried this on your calculator, you found that  $x_n \rightarrow 0.739 \dots$ , no matter where you started. What is this bizarre number? It's the unique solution of the transcendental equation  $x = \cos x$ , and it corresponds to a fixed point of the map. Figure 10.1.3 shows that a typical orbit spirals into the fixed point  $x^* = 0.739 \dots$  as  $n \rightarrow \infty$ . ■

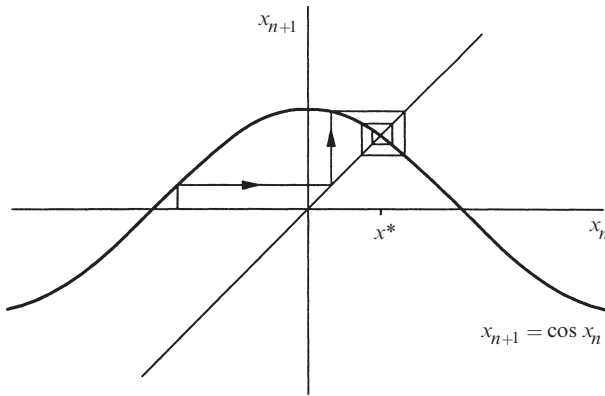


**Figure 10.1.3**

The spiraling motion implies that  $x_n$  converges to  $x^*$  through *damped oscillations*. That is characteristic of fixed points with  $\lambda < 0$ . In contrast, at stable fixed points with  $\lambda > 0$  the convergence is monotonic.

## 10.2 Logistic Map: Numerics

In a fascinating and influential review article, Robert May (1976) emphasized that even simple nonlinear maps could have very complicated dynamics. The article ends memorably with “an evangelical plea for the introduction of these difference equations into elementary mathematics courses, so that students’ intuition may be enriched by seeing the wild things that simple nonlinear equations can do.”

May illustrated his point with the *logistic map*

$$x_{n+1} = rx_n(1 - x_n), \quad (1)$$

a discrete-time analog of the logistic equation for population growth (Section 2.3). Here  $x_n \geq 0$  is a dimensionless measure of the population in the  $n$ th generation and  $r \geq 0$  is the intrinsic growth rate. As shown in Figure 10.2.1, the graph of (1) is a parabola with a maximum value of  $r/4$  at  $x = \frac{1}{2}$ . We restrict the control parameter  $r$  to the range  $0 \leq r \leq 4$  so that (1) maps the interval  $0 \leq x \leq 1$  into itself. (The behavior is much less interesting for other values of  $x$  and  $r$ —see Exercise 10.2.1.)

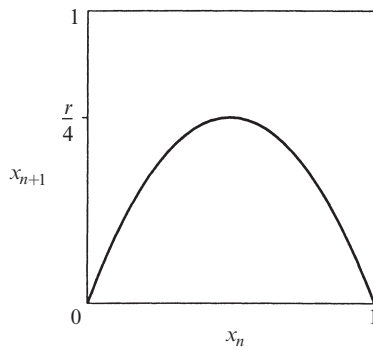


Figure 10.2.1

### Period-Doubling

Suppose we fix  $r$ , choose some initial population  $x_0$ , and then use (1) to generate the subsequent  $x_n$ . What happens?

For small growth rate  $r < 1$ , the population always goes extinct:  $x_n \rightarrow 0$  as  $n \rightarrow \infty$ . This gloomy result can be proven by cobwebbing (Exercise 10.2.2).

For  $1 < r < 3$  the population grows and eventually reaches a nonzero steady state (Figure 10.2.2). The results are plotted here as a *time series* of  $x_n$  vs.  $n$ . To make the sequence clearer, we have connected the discrete points  $(n, x_n)$  by line segments, but remember that only the corners of the jagged curves are meaningful.

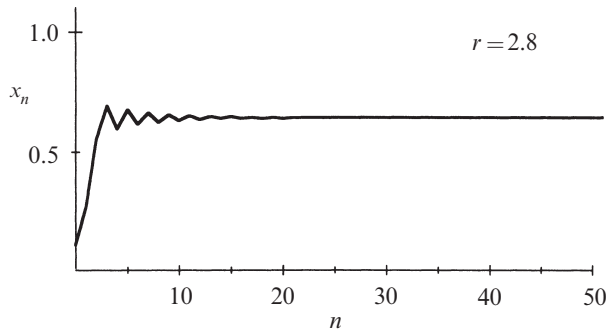


**Figure 10.2.2**

For larger  $r$ , say  $r = 3.3$ , the population builds up again but now *oscillates* about the former steady state, alternating between a large population in one generation and a smaller population in the next (Figure 10.2.3). This type of oscillation, in which  $x_n$  repeats every *two* iterations, is called a **period-2 cycle**.

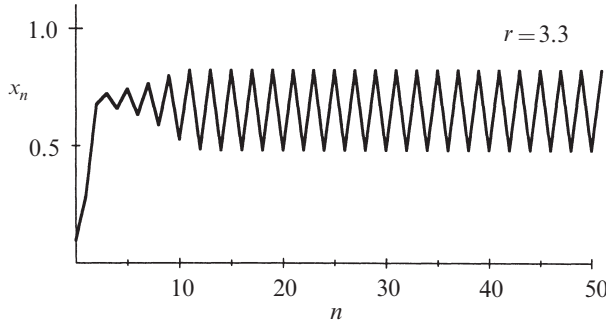


**Figure 10.2.3**

At still larger  $r$ , say  $r = 3.5$ , the population approaches a cycle that now repeats every *four* generations; the previous cycle has doubled its period to **period-4** (Figure 10.2.4).

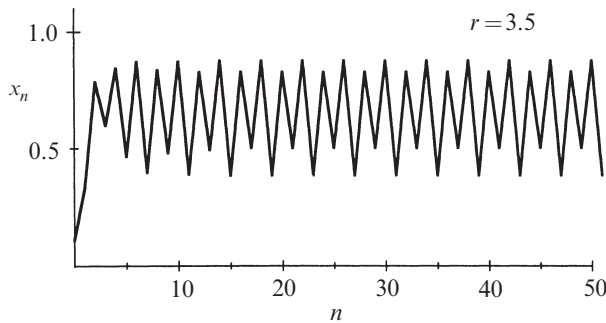


**Figure 10.2.4**

Further **period-doublings** to cycles of period 8, 16, 32, . . . , occur as  $r$  increases. Specifically, let  $r_n$  denote the value of  $r$  where a  $2^n$ -cycle first appears. Then computer experiments reveal that

$r_1 = 3$	(period 2 is born)
$r_2 = 3.449 \dots$	4
$r_3 = 3.54409 \dots$	8
$r_4 = 3.5644 \dots$	16
$r_5 = 3.568759 \dots$	32
$\vdots$	$\vdots$
$r_\infty = 3.569946 \dots$	$\infty$

Note that the successive bifurcations come faster and faster. Ultimately the  $r_n$  converge to a limiting value  $r_\infty$ . The convergence is essentially geometric: in the limit of large  $n$ , the distance between successive transitions shrinks by a constant factor

$$\delta = \lim_{n \rightarrow \infty} \frac{r_n - r_{n-1}}{r_{n+1} - r_n} = 4.669 \dots$$

We'll have a lot more to say about this number in Section 10.6.

### Chaos and Periodic Windows

According to Gleick (1987, p. 69), May wrote the logistic map on a corridor blackboard as a problem for his graduate students and asked, “*What the Christ happens for  $r > r_\infty$ ?*” The answer turns out to be complicated: For many values of  $r$ , the sequence  $\{x_n\}$  never settles down to a fixed point or a periodic orbit—instead the long-term behavior is aperiodic, as in Figure 10.2.5. This is a discrete-time version of the chaos we encountered earlier in our study of the Lorenz equations (Chapter 9).

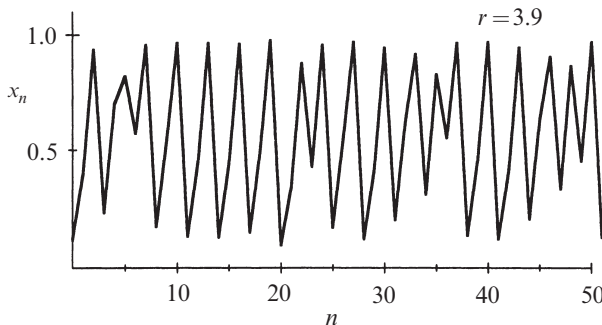


**Figure 10.2.5**

The corresponding cobweb diagram is impressively complex (Figure 10.2.6).

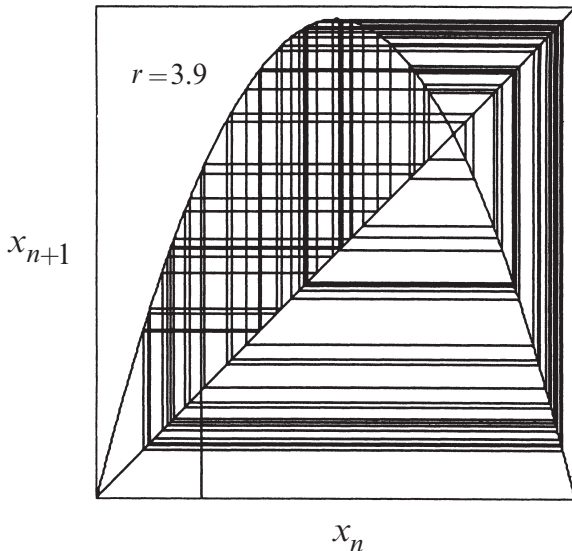


**Figure 10.2.6**

You might guess that the system would become more and more chaotic as  $r$  increases, but in fact the dynamics are more subtle than that. To see the long-term behavior for *all* values of  $r$  at once, we plot the **orbit diagram**, a magnificent picture that has become an icon of nonlinear dynamics (Figure 10.2.7). Figure 10.2.7 plots the system's attractor as a function of  $r$ . To generate the orbit diagram for yourself, you'll need to write a computer program with two "loops." First, choose a value of  $r$ . Then generate an orbit starting from some random initial condition  $x_0$ . Iterate for 300 cycles or so, to allow the system to settle down to its eventual behavior. Once the transients have decayed, plot many points, say  $x_{301}, \dots, x_{600}$  above that  $r$ . Then move to an adjacent value of  $r$  and repeat, eventually sweeping across the whole picture.

Figure 10.2.7 shows the most interesting part of the diagram, in the region  $3.4 \leq r \leq 4$ . At  $r = 3.4$ , the attractor is a period-2 cycle, as indicated by the two branches. As  $r$  increases, both branches split simultaneously, yielding a period-4 cycle. This splitting is the period-doubling bifurcation mentioned earlier. A cascade of further period-doublings occurs as  $r$  increases, yielding period-8, period-16, and so on, until at  $r = r_\infty \approx 3.57$ , the map becomes chaotic and the attractor changes from a finite to an infinite set of points.

For  $r > r_\infty$  the orbit diagram reveals an unexpected mixture of order and chaos, with **periodic windows** interspersed between chaotic clouds of dots. The large window beginning near  $r \approx 3.83$  contains a stable period-3 cycle. A blow-up of part of the period-3 window is shown in the lower panel of Figure 10.2.7. Fantastically, a copy of the orbit diagram reappears in miniature!

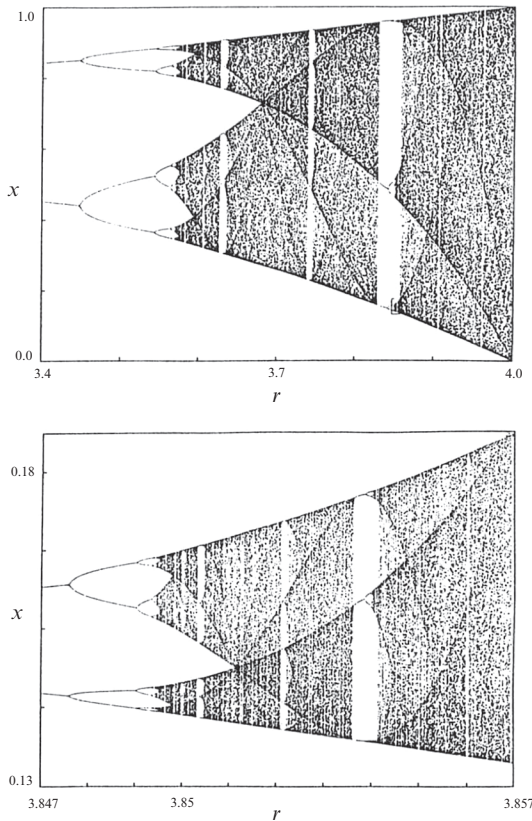


**Figure 10.2.7** Campbell (1979), p. 35, courtesy of Roger Eckhardt

### 10.3 Logistic Map: Analysis

The numerical results of the last section raise many tantalizing questions. Let's try to answer a few of the more straightforward ones.

#### EXAMPLE 10.3.1:

Consider the logistic map  $x_{n+1} = rx_n(1 - x_n)$  for  $0 \leq x_n \leq 1$  and  $0 \leq r \leq 4$ . Find all the fixed points and determine their stability.

*Solution:* The fixed points satisfy  $x^* = f(x^*) = rx^*(1 - x^*)$ . Hence  $x^* = 0$  or  $1 = r(1 - x^*)$ , i.e.,  $x^* = 1 - \frac{1}{r}$ . The origin is a fixed point for all  $r$ , whereas  $x^* = 1 - \frac{1}{r}$  is in the range of allowable  $x$  only if  $r \geq 1$ .

Stability depends on the multiplier  $f'(x^*) = r - 2rx^*$ . Since  $f'(0) = r$ , the origin is stable for  $r < 1$  and unstable for  $r > 1$ . At the other fixed point,

$f'(x^*) = r - 2r(1 - \frac{1}{r}) = 2 - r$ . Hence  $x^* = 1 - \frac{1}{r}$  is stable for  $-1 < (2 - r) < 1$ , i.e., for  $1 < r < 3$ . It is unstable for  $r > 3$ . ■

The results of Example 10.3.1 are clarified by a graphical analysis (Figure 10.3.1). For  $r < 1$  the parabola lies below the diagonal, and the origin is the only fixed point. As  $r$  increases, the parabola gets taller, becoming tangent to the diagonal at  $r = 1$ . For  $r > 1$  the parabola intersects the diagonal in a second fixed point  $x^* = 1 - \frac{1}{r}$ , while the origin loses stability. Thus we see that  $x^*$  bifurcates from the origin in a **transcritical bifurcation** at  $r = 1$  (borrowing a term used earlier for differential equations).

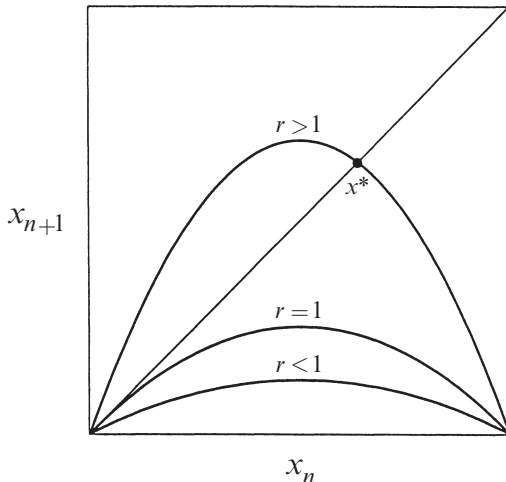


**Figure 10.3.1**

Figure 10.3.1 also suggests how  $x^*$  itself loses stability. As  $r$  increases beyond 1, the slope at  $x^*$  gets increasingly steep. Example 10.3.1 shows that the critical slope  $f'(x^*) = -1$  is attained when  $r = 3$ . The resulting bifurcation is called a **flip bifurcation**.

Flip bifurcations are often associated with period-doubling. In the logistic map, the flip bifurcation at  $r = 3$  does indeed spawn a 2-cycle, as shown in the next example.

### EXAMPLE 10.3.2:

Show that the logistic map has a 2-cycle for all  $r > 3$ .

*Solution:* A 2-cycle exists if and only if there are two points  $p$  and  $q$  such that  $f(p) = q$  and  $f(q) = p$ . Equivalently, such a  $p$  must satisfy  $f(f(p)) = p$ , where  $f(x) = rx(1 - x)$ . Hence  $p$  is a fixed point of the **second-iterate map**

$f^2(x) \equiv f(f(x))$ . Since  $f(x)$  is a quadratic polynomial,  $f^2(x)$  is a quartic polynomial. Its graph for  $r > 3$  is shown in Figure 10.3.2.

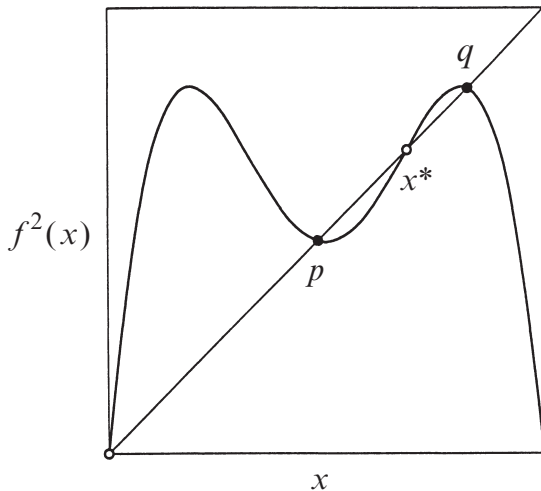


Figure 10.3.2

To find  $p$  and  $q$ , we need to solve for the points where the graph intersects the diagonal, i.e., we need to solve the fourth-degree equation  $f^2(x) = x$ . That sounds hard until you realize that the fixed points  $x^* = 0$  and  $x^* = 1 - \frac{1}{r}$  are trivial solutions of this equation. (They satisfy  $f(x^*) = x^*$ , so  $f^2(x^*) = x^*$  automatically.) After factoring out the fixed points, the problem reduces to solving a quadratic equation.

We outline the algebra involved in the rest of the solution. Expansion of the equation  $f^2(x) - x = 0$  gives  $r^2x(1-x)[1-rx(1-x)] - x = 0$ . After factoring out  $x$  and  $x - (1 - \frac{1}{r})$  by long division, and solving the resulting quadratic equation, we obtain a pair of roots

$$p, q = \frac{r+1 \pm \sqrt{(r-3)(r+1)}}{2r},$$

which are real for  $r > 3$ . Thus a 2-cycle exists for all  $r > 3$ , as claimed. At  $r = 3$ , the roots coincide and equal  $x^* = 1 - \frac{1}{r} = \frac{2}{3}$ , which shows that the 2-cycle bifurcates continuously from  $x^*$ . For  $r < 3$  the roots are complex, which means that a 2-cycle doesn't exist. ■

A cobweb diagram reveals how flip bifurcations can give rise to period-doubling. Consider any map  $f$ , and look at the local picture near a fixed point where  $f'(x^*) \approx -1$  (Figure 10.3.3).

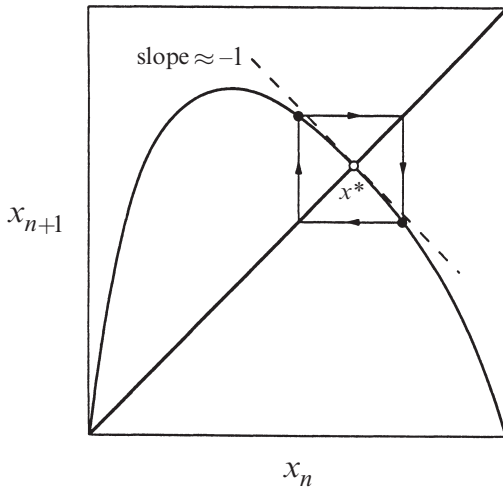


**Figure 10.3.3**

If the graph of  $f$  is concave down near  $x^*$ , the cobweb tends to produce a small, stable 2-cycle close to the fixed point. But like pitchfork bifurcations, flip bifurcations can also be subcritical, in which case the 2-cycle exists *below* the bifurcation and is *unstable*—see Exercise 10.3.11.

The next example shows how to determine the stability of a 2-cycle.

### EXAMPLE 10.3.3:

Show that the 2-cycle of Example 10.3.2 is stable for  $3 < r < 1 + \sqrt{6} = 3.449\dots$ . (This explains the values of  $r_1$  and  $r_2$  found numerically in Section 10.2.)

*Solution:* Our analysis follows a strategy that is worth remembering: To analyze the stability of a cycle, reduce the problem to a question about the stability of a *fixed point*, as follows. Both  $p$  and  $q$  are solutions of  $f^2(x) = x$ , as pointed out in Example 10.3.2; hence  $p$  and  $q$  are *fixed points of the second-iterate map*  $f^2(x)$ . The original 2-cycle is stable precisely if  $p$  and  $q$  are stable fixed points for  $f^2$ .

Now we're on familiar ground. To determine whether  $p$  is a stable fixed point of  $f^2$ , we compute the multiplier

$$\lambda = \frac{d}{dx}(f(f(x)))_{x=p} = f'(f(p))f'(p) = f'(q)f'(p).$$

(Note that the same  $\lambda$  is obtained at  $x = q$ , by the symmetry of the final term above. Hence, when the  $p$  and  $q$  branches bifurcate, they must do so *simultaneously*. We noticed such a simultaneous splitting in our numerical observations of Section 10.2.)

After carrying out the differentiations and substituting for  $p$  and  $q$ , we obtain

$$\begin{aligned}\lambda &= r(1-2q)r(1-2p) \\ &= r^2[1-2(p+q)+4pq] \\ &= r^2[1-2(r+1)/r+4(r+1)/r^2] \\ &= 4+2r-r^2.\end{aligned}$$

Therefore the 2-cycle is linearly stable for  $|4+2r-r^2|<1$ , i.e., for  $3 < r < 1+\sqrt{6}$ . ■

Figure 10.3.4 shows a partial **bifurcation diagram** for the logistic map, based on our results so far. Bifurcation diagrams are different from orbit diagrams in that *unstable* objects are shown as well; orbit diagrams show only the attractors.

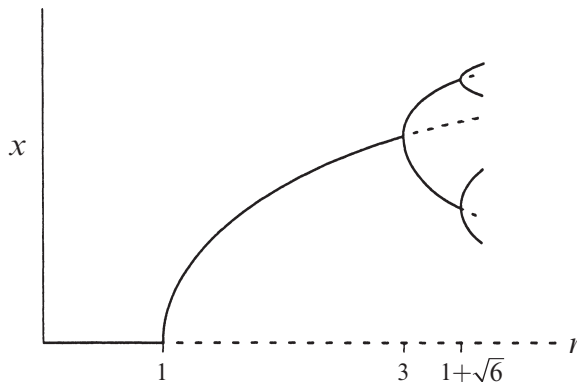


**Figure 10.3.4**

Our analytical methods are becoming unwieldy. A few more exact results can be obtained (see the exercises), but such results are hard to come by. To elucidate the behavior in the interesting region where  $r > r_\infty$ , we are going to rely mainly on graphical and numerical arguments.

## 10.4 Periodic Windows

One of the most intriguing features of the orbit diagram (Figure 10.2.7) is the occurrence of periodic windows for  $r > r_\infty$ . The period-3 window that occurs near  $3.8284 \dots \leq r \leq 3.8415 \dots$  is the most conspicuous. Suddenly, against a backdrop of chaos, a stable 3-cycle appears out of the blue. Our first goal in this section is to understand how this 3-cycle is created. (The same mechanism accounts for the creation of all the other windows, so it suffices to consider this simplest case.)

First, some notation. Let  $f(x) = rx(1-x)$  so that the logistic map is  $x_{n+1} = f(x_n)$ .

Then  $x_{n+2} = f(f(x_n))$  or more simply,  $x_{n+2} = f^2(x_n)$ . Similarly,  $x_{n+3} = f^3(x_n)$ .

The third-iterate map  $f^3(x)$  is the key to understanding the birth of the period-3 cycle. Any point  $p$  in a period-3 cycle repeats every three iterates, by definition, so such points satisfy  $p = f^3(p)$  and are therefore fixed points of the third-iterate map. Unfortunately, since  $f^3(x)$  is an eighth-degree polynomial, we cannot solve for the fixed points explicitly. But a graph provides sufficient insight. Figure 10.4.1 plots  $f^3(x)$  for  $r = 3.835$ .

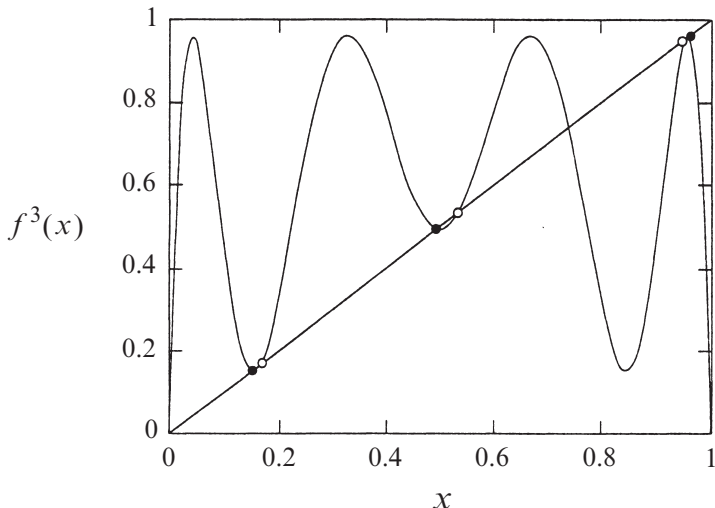


**Figure 10.4.1**

Intersections between the graph and the diagonal line correspond to solutions of  $f^3(x) = x$ . There are eight solutions, six of interest to us and marked with dots, and two imposters that are not genuine period-3; they are actually fixed points, or period-1 points for which  $f(x^*) = x^*$ . The black dots in Figure 10.4.1 correspond to a stable period-3 cycle; note that the slope of  $f^3(x)$  is shallow at these points, consistent with the stability of the cycle. In contrast, the slope exceeds 1 at the cycle marked by the open dots; this 3-cycle is therefore unstable.

Now suppose we decrease  $r$  toward the chaotic regime. Then the graph in Figure 10.4.1 changes shape—the hills move down and the valleys rise up. The curve therefore pulls away from the diagonal. Figure 10.4.2 shows that when  $r = 3.8$ , the six marked intersections have vanished. Hence, for some intermediate value between  $r = 3.8$  and  $r = 3.835$ , the graph of  $f^3(x)$  must have become *tangent* to the diagonal. At this critical value of  $r$ , the stable and unstable period-3 cycles coalesce and annihilate in a **tangent bifurcation**. This transition defines the beginning of the periodic window.

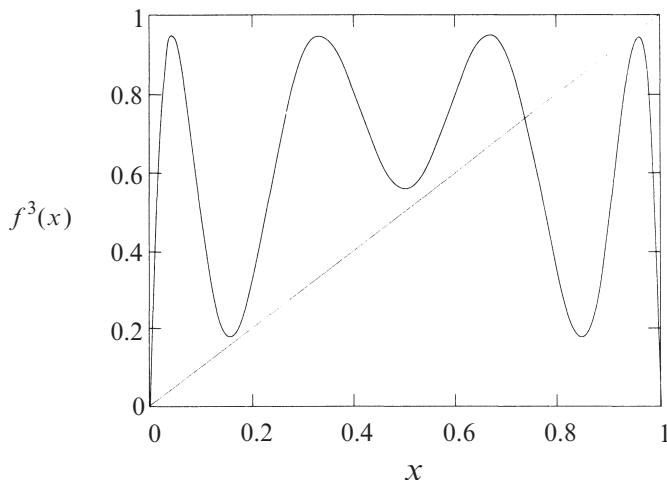


**Figure 10.4.2**

One can show analytically that the value of  $r$  at the tangent bifurcation is  $1 + \sqrt{8} = 3.8284\dots$  (Myrberg 1958). This beautiful result is often mentioned in textbooks and articles—but always without proof. Given the resemblance of this result to the  $1 + \sqrt{6}$  encountered in Example 10.3.3, I'd always assumed it should be comparably easy to derive, and once assigned it as a routine homework problem. Oops! It turns out to be a bear. See Exercise 10.4.10 for hints, and Saha and Strogatz (1994) for Partha Saha's solution, the most elementary one my class could find. Maybe you can do better; if so, let me know!

### Intermittency

For  $r$  just below the period-3 window, the system exhibits an interesting kind of chaos. Figure 10.4.3 shows a typical orbit for  $r = 3.8282$ .

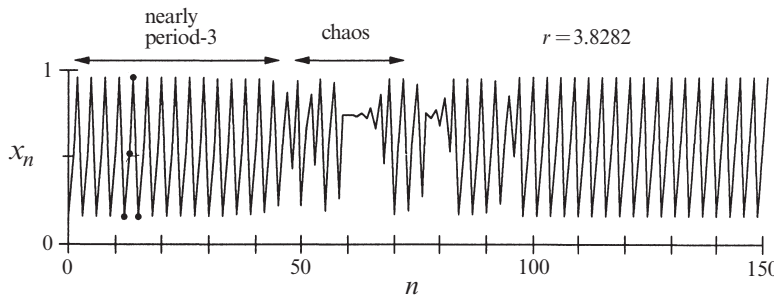


**Figure 10.4.3**

Part of the orbit looks like a stable 3-cycle, as indicated by the black dots. But this is spooky since the 3-cycle no longer exists! We're seeing the *ghost* of the 3-cycle.

We should not be surprised to see ghosts—they *always* occur near saddle-node bifurcations (Sections 4.3 and 8.1) and indeed, a tangent bifurcation is just a saddle-node bifurcation by another name. But the new wrinkle is that the orbit returns to the ghostly 3-cycle repeatedly, with intermittent bouts of chaos between visits. Accordingly, this phenomenon is known as **intermittency** (Pomeau and Manneville 1980).

Figure 10.4.4 shows the geometry underlying intermittency.

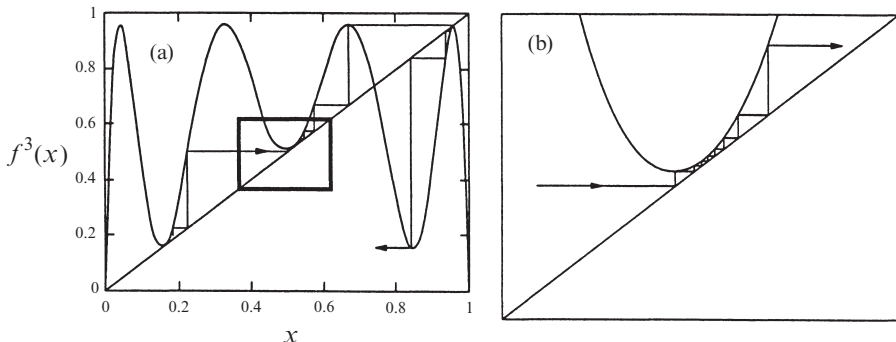


**Figure 10.4.4**

In Figure 10.4.4a, notice the three narrow channels between the diagonal and the graph of  $f^3(x)$ . These channels were formed in the aftermath of the tangent bifurcation, as the hills and valleys of  $f^3(x)$  pulled away from the diagonal. Now focus on the channel in the small box of Figure 10.4.4a, enlarged in Figure 10.4.4b. The orbit takes many iterations to squeeze through the channel. Hence  $f^3(x_n) \approx x_n$  during the passage, and so the orbit looks like a 3-cycle; this explains why we see a ghost.

Eventually, the orbit escapes from the channel. Then it bounces around chaotically until fate sends it back into a channel at some unpredictable later time and place.

Intermittency is not just a curiosity of the logistic map. It arises commonly in systems where the transition from periodic to chaotic behavior takes place by a saddle-node bifurcation of cycles. For instance, Exercise 10.4.8 shows that intermittency can occur in the Lorenz equations. (In fact, it was discovered there; see Pomeau and Manneville 1980).

In experimental systems, intermittency appears as nearly periodic motion interrupted by occasional irregular bursts. The time between bursts is statistically distributed, much like a random variable, even though the system is completely deterministic. As the control parameter is moved farther away from the periodic window, the bursts become more frequent until the system is fully chaotic. This progression is known as the **intermittency route to chaos**.

Figure 10.4.5 shows an experimental example of the intermittency route to chaos in a laser.

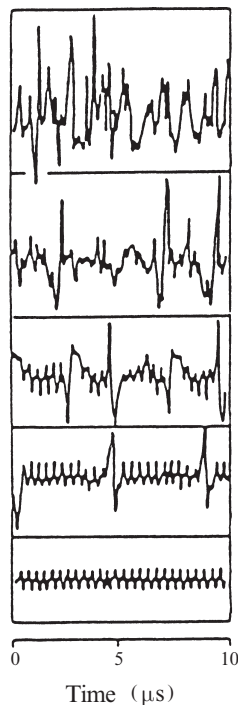


**Figure 10.4.5**

The intensity of the emitted laser light is plotted as a function of time. In the lowest panel of Figure 10.4.5, the laser is pulsing periodically. A bifurcation to intermittency occurs as the system's control parameter (the tilt of the mirror in the laser cavity) is varied. Moving from bottom to top of Figure 10.4.5, we see that the chaotic bursts occur increasingly often.

For a nice review of intermittency in fluids and chemical reactions, see Bergé et al. (1984). Those authors also review two other types of intermittency (the kind considered here is *Type I intermittency*) and give a much more detailed treatment of intermittency in general.

### Period-Doubling in the Window

We commented at the end of Section 10.2 that a copy of the orbit diagram appears in miniature in the period-3 window. The explanation has to do with hills and valleys again. Just after the stable 3-cycle is created in the tangent bifurcation, the slope at the black dots in Figure 10.4.1 is close to +1. As we increase  $r$ , the hills rise and the valleys sink. The slope of  $f^3(x)$  at the black dots decreases steadily

from  $+1$  and eventually reaches  $-1$ . When this occurs, a flip bifurcation causes each of the black dots to split in two; the 3-cycle doubles its period and becomes a 6-cycle. The same mechanism operates here as in the original period-doubling cascade, but now produces orbits of period  $3 \cdot 2^n$ . A similar period-doubling cascade can be found in *all* of the periodic windows.

## 10.5 Liapunov Exponent

We have seen that the logistic map can exhibit aperiodic orbits for certain parameter values, but how do we know that this is really chaos? To be called “chaotic,” a system should also show *sensitive dependence on initial conditions*, in the sense that neighboring orbits separate exponentially fast, on average. In Section 9.3 we quantified sensitive dependence by defining the Liapunov exponent for a chaotic differential equation. Now we extend the definition to one-dimensional maps.

Here’s the intuition. Given some initial condition  $x_0$ , consider a nearby point  $x_0 + \delta_0$ , where the initial separation  $\delta_0$  is extremely small. Let  $\delta_n$  be the separation after  $n$  iterates. If  $|\delta_n| \approx |\delta_0| e^{n\lambda}$ , then  $\lambda$  is called the Liapunov exponent. A positive Liapunov exponent is a signature of chaos.

A more precise and computationally useful formula for  $\lambda$  can be derived. By taking logarithms and noting that  $\delta_n = f^n(x_0 + \delta_0) - f^n(x_0)$ , we obtain

$$\begin{aligned}\lambda &\approx \frac{1}{n} \ln \left| \frac{\delta_n}{\delta_0} \right| \\ &= \frac{1}{n} \ln \left| \frac{f^n(x_0 + \delta_0) - f^n(x_0)}{\delta_0} \right| \\ &= \frac{1}{n} \ln |(f^n)'(x_0)|\end{aligned}$$

where we’ve taken the limit  $\delta_0 \rightarrow 0$  in the last step. The term inside the logarithm can be expanded by the chain rule:

$$(f^n)'(x_0) = \prod_{i=0}^{n-1} f'(x_i) .$$

(We’ve already seen this formula in Example 9.4.1, where it was derived by heuristic reasoning about multipliers, and in Example 10.3.3, for the special case  $n = 2$ .) Hence

$$\begin{aligned}\lambda &\approx \frac{1}{n} \ln \left| \prod_{i=0}^{n-1} f'(x_i) \right| \\ &= \frac{1}{n} \sum_{i=0}^{n-1} \ln |f'(x_i)|.\end{aligned}$$

If this expression has a limit as  $n \rightarrow \infty$ , we define that limit to be the **Liapunov exponent** for the orbit starting at  $x_0$ :

$$\lambda = \lim_{n \rightarrow \infty} \left\{ \frac{1}{n} \sum_{i=0}^{n-1} \ln |f'(x_i)| \right\}.$$

Note that  $\lambda$  depends on  $x_0$ . However, it is the same for all  $x_0$  in the basin of attraction of a given attractor. For stable fixed points and cycles,  $\lambda$  is negative; for chaotic attractors,  $\lambda$  is positive.

The next two examples deal with special cases where  $\lambda$  can be found analytically.

---

### EXAMPLE 10.5.1:

Suppose that  $f$  has a stable  $p$ -cycle containing the point  $x_0$ . Show that the Liapunov exponent  $\lambda < 0$ . If the cycle is superstable, show that  $\lambda = -\infty$ .

*Solution:* As usual, we convert questions about  $p$ -cycles of  $f$  into questions about fixed points of  $f^p$ . Since  $x_0$  is an element of a  $p$ -cycle,  $x_0$  is a fixed point of  $f^p$ . By assumption, the cycle is stable; hence the multiplier  $|f^p)'(x_0)| < 1$ . Therefore  $\ln |(f^p)'(x_0)| < \ln(1) = 0$ , a result that we'll use in a moment.

Next observe that for a  $p$ -cycle,

$$\begin{aligned}\lambda &= \lim_{n \rightarrow \infty} \left\{ \frac{1}{n} \sum_{i=0}^{n-1} \ln |f'(x_i)| \right\} \\ &= \frac{1}{p} \sum_{i=0}^{p-1} \ln |f'(x_i)|\end{aligned}$$

since the same  $p$  terms keep appearing in the infinite sum. Finally, using the chain rule in reverse, we obtain

$$\frac{1}{p} \sum_{i=0}^{p-1} \ln |f'(x_i)| = \frac{1}{p} \ln |(f^p)'(x_0)| < 0,$$

as desired. If the cycle is superstable, then  $|(f^p)'(x_0)| = 0$  by definition, and thus  $\lambda = \frac{1}{p} \ln(0) = -\infty$ . ■

The second example concerns the **tent map**, defined by

$$f(x) = \begin{cases} rx, & 0 \leq x \leq \frac{1}{2} \\ r - rx, & \frac{1}{2} \leq x \leq 1 \end{cases}$$

for  $0 \leq r \leq 2$  and  $0 \leq x \leq 1$  (Figure 10.5.1).

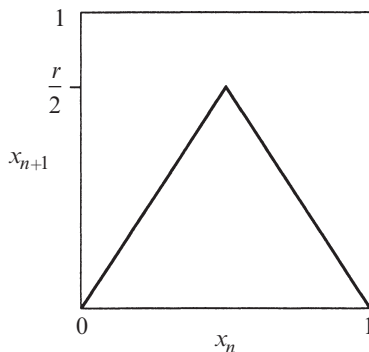


**Figure 10.5.1**

Because it is piecewise linear, the tent map is far easier to analyze than the logistic map.

**EXAMPLE 10.5.2:**

Show that  $\lambda = \ln r$  for the tent map, independent of the initial condition  $x_0$ .

*Solution:* Since  $f'(x) = \pm r$  for all  $x$ , we find  $\lambda = \lim_{n \rightarrow \infty} \left\{ \frac{1}{n} \sum_{i=0}^{n-1} \ln |f'(x_i)| \right\} = \ln r$ . ■

Example 10.5.2 suggests that the tent map has chaotic solutions for all  $r > 1$ , since  $\lambda = \ln r > 0$ . In fact, the dynamics of the tent map can be understood in detail, even in the chaotic regime; see Devaney (1989).

In general, one needs to use a computer to calculate Liapunov exponents. The next example outlines such a calculation for the logistic map.

**EXAMPLE 10.5.3:**

Describe a numerical scheme to compute  $\lambda$  for the logistic map  $f(x) = rx(1 - x)$ . Graph the results as a function of the control parameter  $r$ , for  $3 \leq r \leq 4$ .

*Solution:* Fix some value of  $r$ . Then, starting from a random initial condition, iterate the map long enough to allow transients to decay, say 300 iterates or so. Next compute a large number of additional iterates, say 10,000. You only need to store the current value of  $x_n$ , not all the previous iterates. Compute  $\ln |f'(x_n)| = \ln |r - 2rx_n|$  and add it to the sum of the previous logarithms. The Liapunov exponent is then obtained by dividing the grand total by 10,000. Repeat this procedure for the next  $r$ , and so on. The end result should look like Figure 10.5.2.

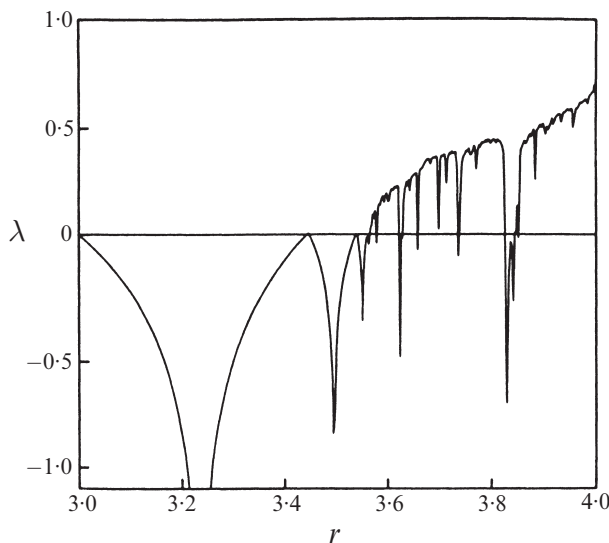


**Figure 10.5.2** Olsen and Degn (1985), p. 175

Comparing this graph to the orbit diagram (Figure 10.2.7), we notice that  $\lambda$  remains negative for  $r < r_{\infty} \approx 3.57$ , and approaches zero at the period-doubling bifurcations. The negative spikes correspond to the  $2^n$ -cycles. The onset of chaos is visible near  $r \approx 3.57$ , where  $\lambda$  first becomes positive. For  $r > 3.57$  the Liapunov exponent generally increases, except for the dips caused by the windows of periodic behavior. Note the large dip due to the period-3 window near  $r = 3.83$ . ■

Actually, all the dips in Figure 10.5.2 should drop down to  $\lambda = -\infty$ , because a superstable cycle is guaranteed to occur somewhere near the middle of each dip, and such cycles have  $\lambda = -\infty$ , by Example 10.5.1. This part of the spike is too narrow to be resolved in Figure 10.5.2.

## 10.6 Universality and Experiments

This section deals with some of the most astonishing results in all of nonlinear dynamics. The ideas are best introduced by way of an example.

### EXAMPLE 10.6.1:

Plot the graph of the **sine map**  $x_{n+1} = r \sin \pi x_n$  for  $0 \leq r \leq 1$  and  $0 \leq x \leq 1$ , and compare it to the logistic map. Then plot the orbit diagrams for both maps, and list some similarities and differences.

*Solution:* The graph of the sine map is shown in Figure 10.6.1.

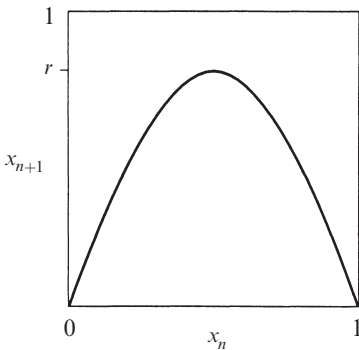


**Figure 10.6.1**

It has the same shape as the graph of the logistic map. Both curves are smooth, concave down, and have a single maximum. Such maps are called **unimodal**.

Figure 10.6.2 shows the orbit diagrams for the sine map (top panel) and the logistic map (bottom panel). The resemblance is incredible. Note that both diagrams have the same vertical scale, but that the horizontal axis of the sine map diagram is scaled by a factor of 4. This normalization is appropriate because the maximum of  $r \sin \pi x$  is  $r$ , whereas that of  $rx(1 - x)$  is  $\frac{1}{4}r$ .

Figure 10.6.2 shows that the *qualitative* dynamics of the two maps are identical. They both undergo period-doubling routes to chaos, followed by periodic windows interwoven with chaotic bands. Even more remarkably, the periodic windows occur in the same order, and with the same relative sizes. For instance, the period-3 window is the largest in both cases, and the next largest windows preceding it are period-5 and period-6.

But there are *quantitative* differences. For instance, the period-doubling bifurcations occur later in the logistic map, and the periodic windows are thinner. ■

### Qualitative Universality: The U-sequence

Example 10.6.1 illustrates a powerful theorem due to Metropolis et al. (1973). They considered all unimodal maps of the form  $x_{n+1} = rf(x_n)$ , where  $f(x)$  also satisfies  $f(0) = f(1) = 0$ . (For the precise conditions, see their original paper.) Metropolis et al. proved that as  $r$  is varied, the order in which stable periodic solutions appear is *independent* of the unimodal map being iterated. That is, *the periodic attractors always occur in the same sequence*, now called the universal or **U-sequence**. This amazing result implies that the algebraic form of  $f(x)$  is irrelevant; only its overall shape matters.

Up to period 6, the U-sequence is

$$1, 2, 2 \times 2, 6, 5, 3, 2 \times 3, 5, 6, 4, 6, 5, 6.$$

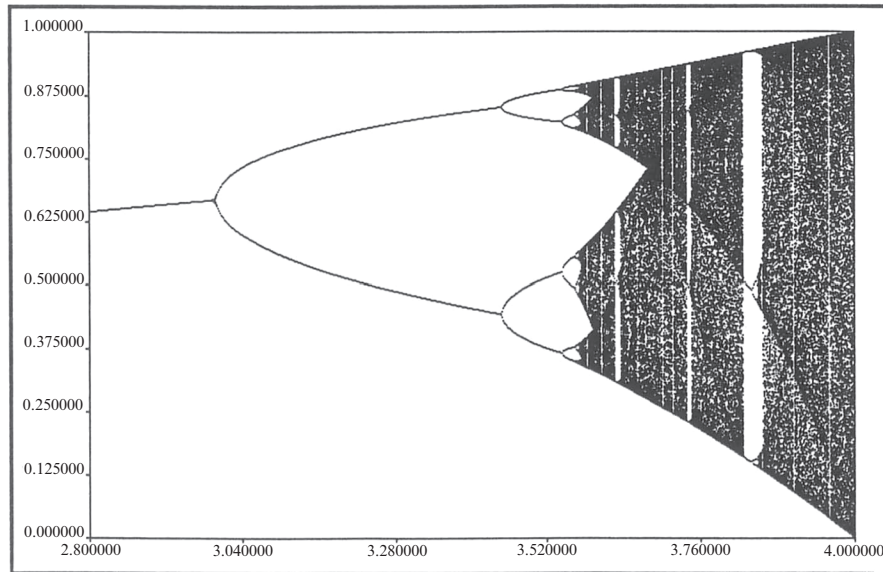
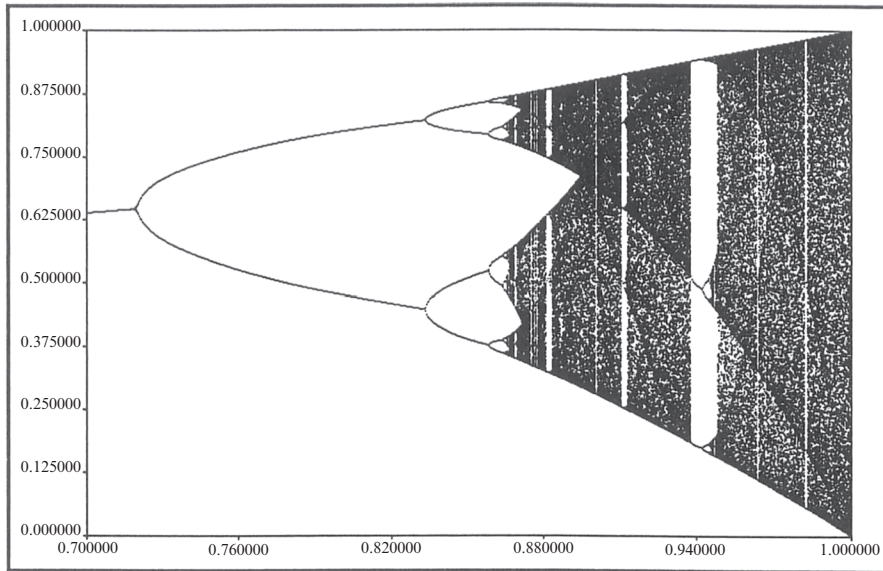


**Figure 10.6.2** Courtesy of Andy Christian

The beginning of this sequence is familiar: periods 1, 2, and  $2 \times 2$  are the first stages in the period-doubling scenario. (The later period-doublings give periods greater than 6, so they are omitted here.) Next, periods 6, 5, 3 correspond to the large windows mentioned in the discussion of Figure 10.6.2. Period  $2 \times 3$  is the first period-doubling of the period-3 cycle. The later cycles 5, 6, 4, 6, 5, 6 are less

familiar; they occur in tiny windows and easy to miss (see Exercise 10.6.5 for their locations in the logistic map).

The U-sequence has been found in experiments on the Belousov-Zhabotinsky chemical reaction. Simoyi et al. (1982) studied the reaction in a continuously stirred flow reactor and found a regime in which periodic and chaotic states alternate as the flow rate is increased. Within the experimental resolution, the periodic states occurred in the exact order predicted by the U-sequence. See Section 12.4 for more details of these experiments.

The U-sequence is qualitative; it dictates the order, but not the precise parameter values, at which periodic attractors occur. We turn now to Mitchell Feigenbaum's celebrated discovery of *quantitative* universality in one-dimensional maps.

### Quantitative Universality

You should read the dramatic story behind this work in Gleick (1987), and also see Feigenbaum (1980; reprinted in Cvitanovic 1989a) for his own reminiscences. The original technical papers are Feigenbaum (1978, 1979)—published only after being rejected by other journals. These papers are fairly heavy reading; see Feigenbaum (1980), Schuster (1989) and Cvitanovic (1989b) for more accessible expositions.

Here's a capsule history. Around 1975, Feigenbaum began to study period-doubling in the logistic map. First he developed a complicated (and now forgotten) "generating function theory" to predict  $r_n$ , the value of  $r$  where a  $2^n$ -cycle first appears. To check his theory numerically, and not being fluent with large computers, he programmed his handheld calculator to compute the first several  $r_n$ . As the calculator chugged along, Feigenbaum had time to guess where the next bifurcation would occur. He noticed a simple rule: the  $r_n$  converged geometrically, with the distance between successive transitions shrinking by a constant factor of about 4.669.

Feigenbaum (1980) recounts what happened next:

I spent part of a day trying to fit the convergence rate value, 4.669, to the mathematical constants I knew. The task was fruitless, save for the fact that it made the number memorable.

At this point I was reminded by Paul Stein that period-doubling isn't a unique property of the quadratic map but also occurs, for example, in  $x_{n+1} = r \sin \pi x_n$ . However my generating function theory rested heavily on the fact that the nonlinearity was simply quadratic and not transcendental. Accordingly, my interest in the problem waned.

Perhaps a month later I decided to compute the  $r_n$ 's in the transcendental case numerically. This problem was even slower to compute than the quadratic one. Again, it became apparent that the  $r_n$ 's converged geometrically, and altogether amazingly, the convergence rate was the same 4.669 that I remembered by virtue of my efforts to fit it.

In fact, the same convergence rate appears *no matter what unimodal map is iterated!* In this sense, the number

$$\delta = \lim_{n \rightarrow \infty} \frac{r_n - r_{n-1}}{r_{n+1} - r_n} = 4.669\dots$$

is ***universal***. It is a new mathematical constant, as basic to period-doubling as  $\pi$  is to circles.

Figure 10.6.3 schematically illustrates the meaning of  $\delta$ . Let  $\Delta_n = r_n - r_{n+1}$  denote the distance between consecutive bifurcation values. Then  $\Delta_n / \Delta_{n+1} \rightarrow \delta$  as  $n \rightarrow \infty$ .

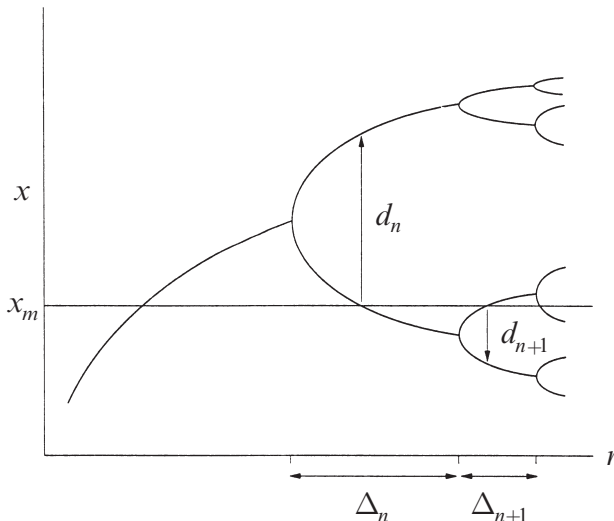


**Figure 10.6.3**

There is also universal scaling in the  $x$ -direction. It is harder to state precisely because the pitchforks have varying widths, even at the same value of  $r$ . (Look back at the orbit diagrams in Figure 10.6.2 to confirm this.) To take account of this nonuniformity, we define a standard  $x$ -scale as follows: Let  $x_m$  denote the maximum of  $f$ , and let  $d_n$  denote the distance from  $x_m$  to the *nearest* point in a  $2^n$ -cycle (Figure 10.6.3).

Then the ratio  $d_n / d_{n+1}$  tends to a universal limit as  $n \rightarrow \infty$ :

$$\frac{d_n}{d_{n+1}} \rightarrow \alpha = -2.5029\dots,$$

independent of the precise form of  $f$ . Here the negative sign indicates that the nearest point in the  $2^n$ -cycle is alternately above and below  $x_m$ , as shown in Figure 10.6.3. Thus the  $d_n$  are alternately positive and negative.

Feigenbaum went on to develop a beautiful theory that explained why  $\alpha$  and  $\delta$  are universal (Feigenbaum 1979). He borrowed the idea of renormalization from statistical physics, and thereby found an analogy between  $\alpha$ ,  $\delta$  and the universal exponents observed in experiments on second-order phase transitions in magnets, fluids, and other physical systems (Ma 1976). In Section 10.7, we give a brief look at this renormalization theory.

### Experimental Tests

Since Feigenbaum's work, sequences of period-doubling bifurcations have been measured in a variety of experimental systems. For instance, in the convection experiment of Libchaber et al. (1982), a box containing liquid mercury is heated from below. The control parameter is the Rayleigh number  $R$ , a dimensionless measure of the externally imposed temperature gradient from bottom to top. For  $R$  less than a critical value  $R_c$ , heat is conducted upward while the fluid remains motionless. But for  $R > R_c$ , the motionless state becomes unstable and **convection** occurs—hot fluid rises on one side, loses its heat at the top, and descends on the other side, setting up a pattern of counterrotating cylindrical **rolls** (Figure 10.6.4).

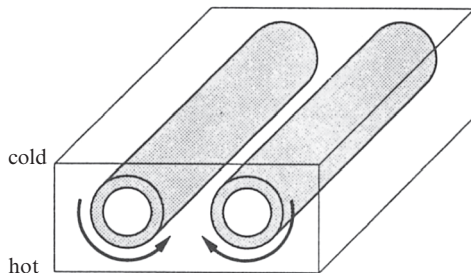


Figure 10.6.4

For  $R$  just slightly above  $R_c$ , the rolls are straight and the motion is steady. Furthermore, at any fixed location in space, the temperature is constant. With more heating, another instability sets in. A wave propagates back and forth along each roll, causing the temperature to oscillate at each point.

In traditional experiments of this sort, one keeps turning up the heat, causing further instabilities to occur until eventually the roll structure is destroyed and the system becomes turbulent. Libchaber et al. (1982) wanted to be able to increase the heat *without* destabilizing the spatial structure. That's why they chose mercury—then the roll structure could be stabilized by applying a dc magnetic field to the whole system. Mercury has a high electrical conductivity, so there is a strong tendency for the rolls to align with the field, thereby retaining their spatial

organization. There are further niceties in the experimental design, but they need not concern us; see Libchaber et al. (1982) or Bergé et al. (1984).

Now for the experimental results. Figure 10.6.5 shows that this system undergoes a sequence of period-doublings as the Rayleigh number is increased.

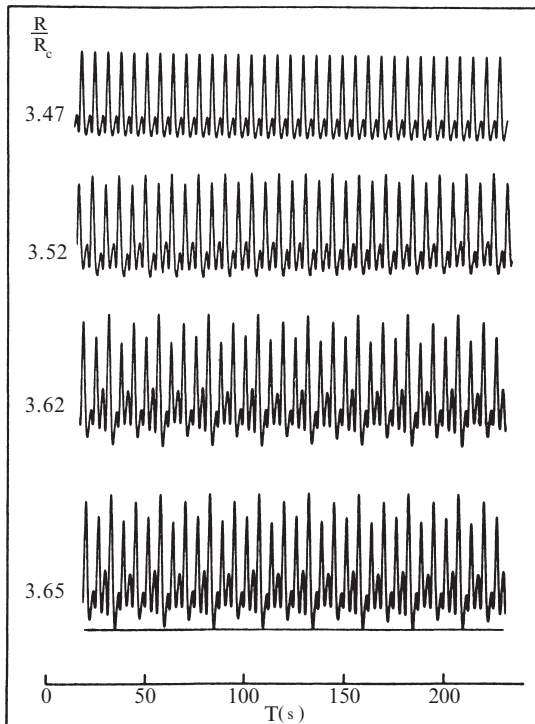


**Figure 10.6.5** Libchaber et al. (1982), p.213

Each time series shows the temperature variations at one point in the fluid. For  $R/R_c = 3.47$ , the temperature varies periodically. This may be regarded as the basic period-1 state. When  $R$  is increased to  $R/R_c = 3.52$ , the successive temperature maxima are no longer equal; the odd peaks are a little higher than before, and the even peaks are a little lower. This is the period-2 state. Further increases in  $R$  generate additional period-doublings, as shown in the lower two time series in Figure 10.6.5.

By carefully measuring the values of  $R$  at the period-doubling bifurcations, Libchaber et al. (1982) arrived at a value of  $\delta = 4.4 \pm 0.1$ , in reasonable agreement with the theoretical result  $\delta \approx 4.699$ .

Table 10.6.1, adapted from Cvitanovic (1989b), summarizes the results from a few experiments on fluid convection and nonlinear electronic circuits. The experimental estimates of  $\delta$  are shown along with the errors quoted by the experimentalists; thus 4.3 (8) means  $4.3 \pm 0.8$ .

Experiment	Number of period doublings	$\delta$	Authors
<i>Hydrodynamic</i>			
water	4	4.3(8)	Giglio et al. (1981)
mercury	4	4.4(1)	Libchaber et al. (1982)
<i>Electronic</i>			
diode	4	4.5(6)	Linsay (1981)
diode	5	4.3(1)	Testa et al. (1982)
transistor	4	4.7(3)	Arecchi and Lisi (1982)
Josephson simul.	3	4.5(3)	Yeh and Kao (1982)

**Table 10.6.1**

It is important to understand that these measurements are difficult. Since  $\delta \approx 5$ , each successive bifurcation requires about a fivefold improvement in the experimenter's ability to measure the external control parameter. Also, experimental noise tends to blur the structure of high-period orbits, so it is hard to tell precisely when a bifurcation has occurred. In practice, one cannot measure more than about five period-doublings. Given these difficulties, the agreement between theory and experiment is impressive.

Period-doubling has also been measured in laser, chemical, and acoustic systems, in addition to those listed here. See Cvitanovic (1989b) for references.

### What Do 1-D Maps Have to Do with Science?

The predictive power of Feigenbaum's theory may strike you as mysterious. How can the theory work, given that it includes none of the *physics* of real systems like convecting fluids or electronic circuits? And real systems often have tremendously many degrees of freedom—how can all that complexity be captured by a one-dimensional map? Finally, real systems evolve in continuous time, so how can a theory based on discrete-time maps work so well?

To work toward the answer, let's begin with a system that is simpler than a convecting fluid, yet (seemingly) more complicated than a one-dimensional map. The system is a set of three differential equations concocted by Rössler (1976) to exhibit the simplest possible strange attractor. The **Rössler system** is

$$\begin{aligned}\dot{x} &= -y - z \\ \dot{y} &= x + ay \\ \dot{z} &= b + z(x - c)\end{aligned}$$

where  $a$ ,  $b$ , and  $c$  are parameters. This system contains only one nonlinear term,  $zx$ , and is even simpler than the Lorenz system (Chapter 9), which has two nonlinearities.

Figure 10.6.6 shows two-dimensional projections of the system's attractor for different values of  $c$  (with  $a = b = 0.2$  held fixed).

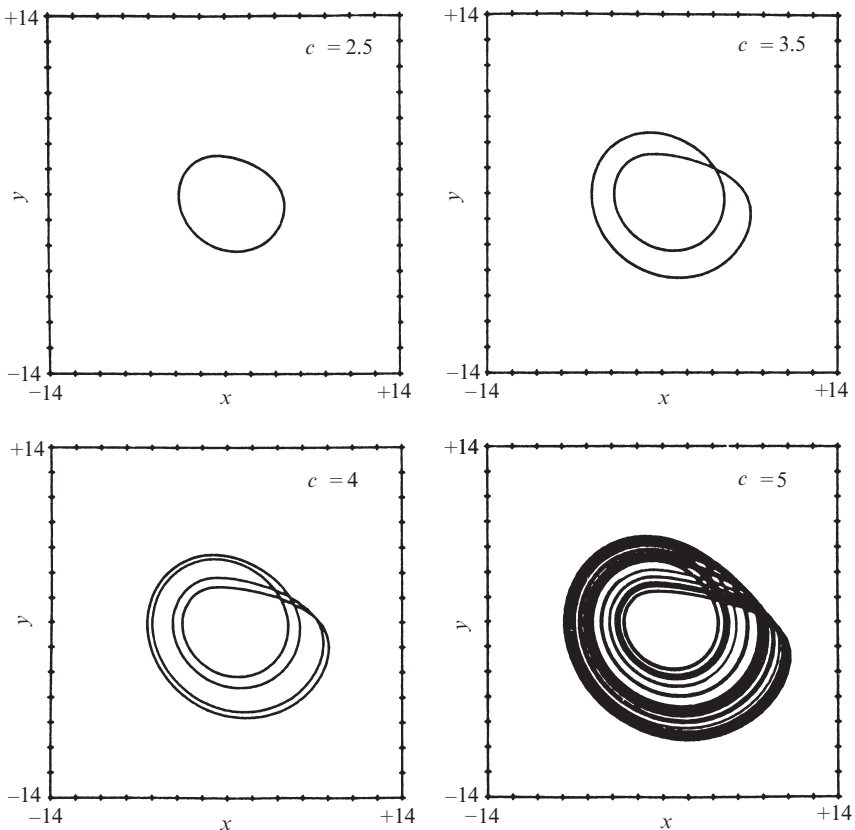


**Figure 10.6.6** Olsen and Degn (1985), p.185

At  $c = 2.5$  the attractor is a simple limit cycle. As  $c$  is increased to 3.5, the limit cycle goes around twice before closing, and its period is approximately twice that of the original cycle. This is what period-doubling looks like in a continuous-time system! In fact, somewhere between  $c = 2.5$  and 3.5, a **period-doubling bifurcation of cycles** must have occurred. (As Figure 10.6.6 suggests, such a bifurcation can occur only in three or higher dimensions, since the limit cycle needs room to avoid crossing itself.) Another period-doubling bifurcation creates the four-loop cycle shown at  $c = 4$ . After an infinite cascade of further period-doublings, one obtains the strange attractor shown at  $c = 5$ .

To compare these results to those obtained for one-dimensional maps, we use Lorenz's trick for obtaining a map from a flow (Section 9.4). For a given value of  $c$ , we record the successive local maxima of  $x(t)$  for a trajectory on the strange attractor. Then we plot  $x_{n+1}$  vs.  $x_n$ , where  $x_n$  denotes the  $n$ th local maximum. This

Lorenz map for  $c = 5$  is shown in Figure 10.6.7. The data points fall very nearly on a one-dimensional curve. Note the uncanny resemblance to the logistic map!

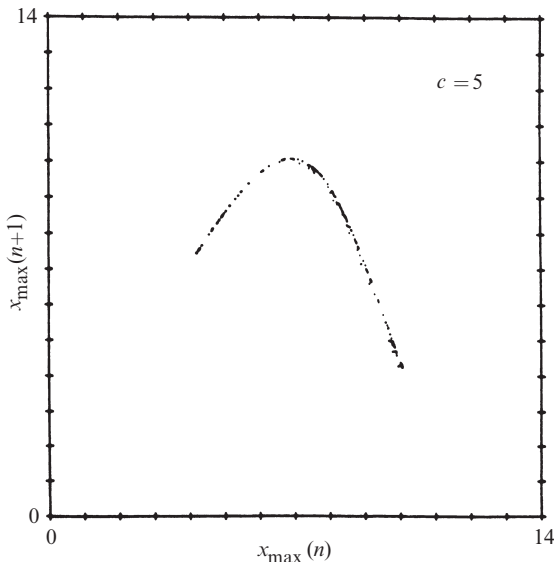


**Figure 10.6.7** Olsen and Degn (1985), p.186

We can even compute an orbit diagram for the Rössler system. Now we allow all values of  $c$ , not just those where the system is chaotic. Above each  $c$ , we plot *all* the local maxima  $x_n$  on the attractor for that value of  $c$ . The number of different maxima tells us the “period” of the attractor. For instance, at  $c = 3.5$  the attractor is period-2 (Figure 10.6.6), and hence there are two local maxima of  $x(t)$ . Both of these points are graphed above  $c = 3.5$  in Figure 10.6.8. We proceed in this way for all values of  $c$ , thereby sweeping out the orbit diagram.

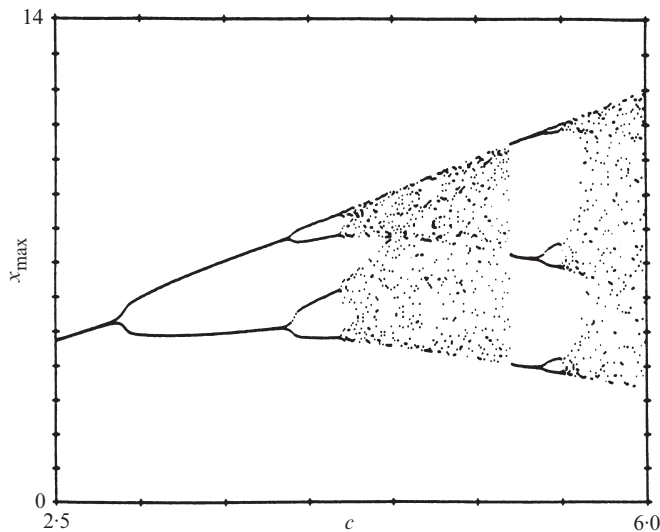


**Figure 10.6.8** Olsen and Degn (1985), p.186

This orbit diagram allows us to keep track of the bifurcations in the Rössler system. We see the period-doubling route to chaos and the large period-3 window—all our old friends are here.

Now we can see why certain physical systems are governed by Feigenbaum's universality theory—if the system's Lorenz map is nearly one-dimensional and unimodal, then the theory applies. This is certainly the case for the Rössler system, and probably for Libchaber's convecting mercury. But not all systems have one-dimensional Lorenz maps. For the Lorenz map to be almost one-dimensional, the strange attractor has to be very flat, i.e., only slightly more than two-dimensional. This requires that the system be highly dissipative; only two or three degrees of freedom are truly active, and the rest follow along slavishly. (Incidentally, that's another reason why Libchaber et al. (1982) applied a magnetic field; it increases the damping in the system, and thereby favors a low-dimensional brand of chaos.)

So while the theory works for some mildly chaotic systems, it does not apply to fully turbulent fluids or fibrillating hearts, where there are many active degrees of freedom corresponding to complicated behavior in space as well as time. We are still a long way from understanding such systems.

## 10.7 Renormalization

In this section we give an intuitive introduction to Feigenbaum's (1979) renormalization theory for period-doubling. For nice expositions at a higher mathematical level than that presented here, see Feigenbaum (1980), Collet and Eckmann (1980), Schuster (1989), Drazin (1992), and Cvitanovic (1989b).

First we introduce some notation. Let  $f(x, r)$  denote a unimodal map that undergoes a period-doubling route to chaos as  $r$  increases, and suppose that  $x_m$  is the maximum of  $f$ . Let  $r_n$  denote the value of  $r$  at which a  $2^n$ -cycle is born, and let  $R_n$  denote the value of  $r$  at which the  $2^n$ -cycle is superstable.

Feigenbaum phrased his analysis in terms of the superstable cycles, so let's get some practice with them.

### EXAMPLE 10.7.1:

Find  $R_0$  and  $R_1$  for the map  $f(x, r) = r - x^2$ .

*Solution:* At  $R_0$  the map has a superstable fixed point, by definition. The fixed point condition is  $x^* = R_0 - (x^*)^2$  and the superstability condition is  $\lambda = (\partial f / \partial x)_{x=x^*} = 0$ . Since  $\partial f / \partial x = -2x$ , we must have  $x^* = 0$ , i.e., the fixed point is the maximum of  $f$ . Substituting  $x^* = 0$  into the fixed point condition yields  $R_0 = 0$ .

At  $R_1$  the map has a superstable 2-cycle. Let  $p$  and  $q$  denote the points of the cycle. Superstability requires that the multiplier  $\lambda = (-2p)(-2q) = 0$ , so the point  $x = 0$  must be one of the points in the 2-cycle. Then the period-2 condition  $f^2(0, R_1) = 0$  implies  $R_1 - (R_1)^2 = 0$ . Hence  $R_1 = 1$  (since the other root gives a fixed point, not a 2-cycle). ■

Example 10.7.1 illustrates a general rule: A superstable cycle of a unimodal map always contains  $x_m$  as one of its points. Consequently, there is a simple graphical way to locate  $R_n$  (Figure 10.7.1). We draw a horizontal line at height  $x_m$ ; then  $R_n$  occurs where this line intersects the *figtree* portion of the orbit diagram (Feigenbaum = *figtree* in German). Note that  $R_n$  lies between  $r_n$  and  $r_{n+1}$ . Numerical experiments show that the spacing between successive  $R_n$  also shrinks by the universal factor  $\delta \approx 4.669$ .

The renormalization theory is based on the *self-similarity* of the figtree—the twigs look like the earlier branches, except they are scaled down in both the  $x$  and  $r$  directions. This structure reflects the endless repetition of the same dynamical processes; a  $2^n$ -cycle is born, then becomes superstable, and then loses stability in a period-doubling bifurcation.

To express the self-similarity mathematically, we compare  $f$  with its second iterate  $f^2$  at corresponding values of  $r$ , and then “renormalize” one map into the other. Specifically, look at the graphs of  $f(x, R_0)$  and  $f^2(x, R_1)$  (Figure 10.7.2, a and b).

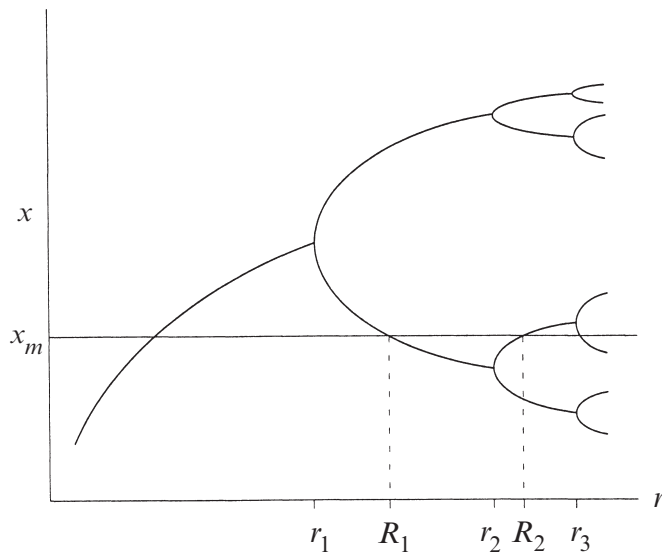


**Figure 10.7.1**

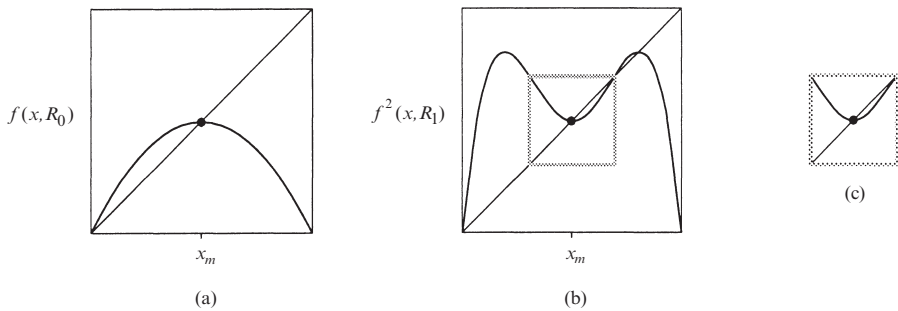


**Figure 10.7.2**

This is a fair comparison because the maps have the same stability properties:  $x_m$  is a superstable fixed point for both of them. Please notice that to obtain Figure 10.7.2b, we took the second iterate of  $f$  and increased  $r$  from  $R_0$  to  $R_1$ . This  $r$ -shifting is a basic part of the renormalization procedure.

The small box of Figure 10.7.2b is reproduced in Figure 10.7.2c. The key point is that Figure 10.7.2c looks practically identical to Figure 10.7.2a, except for a change of scale and a reversal of both axes. From the point of view of dynamics, the two maps are very similar—cobweb diagrams starting from corresponding points would look almost the same.

Now we need to convert these qualitative observations into formulas. A helpful first step is to translate the origin of  $x$  to  $x_m$ , by redefining  $x$  as  $x - x_m$ . This

redefinition of  $x$  dictates that we also subtract  $x_m$  from  $f$ , since  $f(x_n, r) = x_{n+1}$ . The translated graphs are shown in Figure 10.7.3a and 10.7.3b.

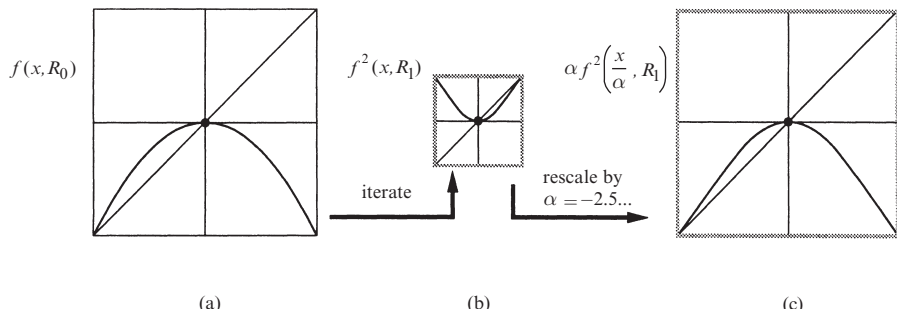


**Figure 10.7.3**

Next, to make Figure 10.7.3b look like Figure 10.7.3a, we blow it up by a factor  $|\alpha| > 1$  in both directions, and also invert it by replacing  $(x, y)$  by  $(-x, -y)$ . Both operations can be accomplished in one step if we define the *scale factor*  $\alpha$  to be *negative*. As you are asked to show in Exercise 10.7.2, rescaling by  $\alpha$  is equivalent to replacing  $f^2(x, R_1)$  by  $\alpha f^2(x/\alpha, R_1)$ . Finally, the resemblance between Figure 10.7.3a and Figure 10.7.3c shows that

$$f(x, R_0) \approx \alpha f^2\left(\frac{x}{\alpha}, R_1\right).$$

In summary,  $f$  has been *renormalized* by taking its second iterate, rescaling  $x \rightarrow x/\alpha$ , and shifting  $r$  to the next superstable value.

There is no reason to stop at  $f^2$ . For instance, we can renormalize  $f^2$  to generate  $f^4$ ; it too has a superstable fixed point if we shift  $r$  to  $R_2$ . The same reasoning as above yields

$$f^2\left(\frac{x}{\alpha}, R_1\right) \approx \alpha f^4\left(\frac{x}{\alpha^2}, R_2\right).$$

When expressed in terms of the original map  $f(x, R_0)$ , this equation becomes

$$f(x, R_0) \approx \alpha^2 f^4\left(\frac{x}{\alpha^2}, R_2\right).$$

After renormalizing  $n$  times we get

$$f(x, R_0) \approx \alpha^n f^{(2^n)}\left(\frac{x}{\alpha^n}, R_n\right).$$

Feigenbaum found numerically that

$$\lim_{n \rightarrow \infty} \alpha^n f^{(2^n)} \left( \frac{x}{\alpha^n}, R_n \right) = g_0(x), \quad (1)$$

where  $g_0(x)$  is a ***universal function*** with a superstable fixed point. The limiting function exists only if  $\alpha$  is chosen correctly, specifically,  $\alpha = -2.5029\dots$

Here “universal” means that the limiting function  $g_0(x)$  is independent of the original  $f$  (almost). This seems incredible at first, but the form of (1) suggests the explanation:  $g_0(x)$  depends on  $f$  only through its behavior near  $x = 0$ , since that’s all that survives in the argument  $x/\alpha^n$  as  $n \rightarrow \infty$ . With each renormalization, we’re blowing up a smaller and smaller neighborhood of the maximum of  $f$ , so practically all information about the global shape of  $f$  is lost.

One caveat: The *order* of the maximum is never forgotten. Hence a more precise statement is that  $g_0(x)$  is universal for all  $f$  with a quadratic maximum (the generic case). A different  $g_0(x)$  is found for  $f$ ’s with a fourth-degree maximum, etc.

To obtain other universal functions  $g_i(x)$ , start with  $f(x, R_i)$  instead of  $f(x, R_0)$ :

$$g_i(x) = \lim_{n \rightarrow \infty} \alpha^n f^{(2^n)} \left( \frac{x}{\alpha^n}, R_{n+i} \right).$$

Here  $g_i(x)$  is a universal function with a superstable  $2^i$ -cycle. The case where we start with  $R_i = R_\infty$  (at the onset of chaos) is the most interesting and important, since then

$$f(x, R_\infty) \approx \alpha f^2 \left( \frac{x}{\alpha}, R_\infty \right).$$

For once, we don’t have to shift  $r$  when we renormalize! The limiting function  $g_\infty(x)$ , usually called  $g(x)$ , satisfies

$$g(x) = \alpha g^2 \left( \frac{x}{\alpha} \right). \quad (2)$$

This is a ***functional equation*** for  $g(x)$  and the universal scale factor  $\alpha$ . It is self-referential:  $g(x)$  is defined in terms of itself.

The functional equation is not complete until we specify boundary conditions on  $g(x)$ . After the shift of origin, all our unimodal  $f$ ’s have a maximum at  $x = 0$ , so we require  $g'(0) = 0$ . Also, we can set  $g(0) = 1$  without loss of generality. (This just defines the scale for  $x$ ; if  $g(x)$  is a solution of (2), so is  $\mu g(x/\mu)$ , with the same  $\alpha$ . See Exercise 10.7.3.)

Now we solve for  $g(x)$  and  $\alpha$ . At  $x=0$  the functional equation gives  $g(0) = \alpha g(g(0))$ . But  $g(0) = 1$ , so  $1 = \alpha g(1)$ . Hence,

$$\alpha = 1/g(1),$$

which shows that  $\alpha$  is determined by  $g(x)$ . No one has ever found a closed form solution for  $g(x)$ , so we resort to a power series solution

$$g(x) = 1 + c_2 x^2 + c_4 x^4 + \dots$$

(which assumes that the maximum is quadratic). The coefficients are determined by substituting the power series into (2) and matching like powers of  $x$ . Feigenbaum (1979) used a seven-term expansion, and found  $c_2 \approx -1.5276$ ,  $c_4 \approx 0.1048$ , along with  $\alpha \approx -2.5029$ . Thus the renormalization theory has succeeded in explaining the value of  $\alpha$  observed numerically.

The theory also explains the value of  $\delta$ . Unfortunately, that part of the story requires more sophisticated apparatus than we are prepared to discuss (operators in function space, Frechet derivatives, etc.). Instead we turn now to a concrete example of renormalization. The calculations are only approximate, but they can be done explicitly, using algebra instead of functional equations.

### Renormalization for Pedestrians

The following pedagogical calculation is intended to clarify the renormalization process. As a bonus, it gives closed form approximations for  $\alpha$  and  $\delta$ . Our treatment is modified from May and Oster (1980) and Helleman (1980).

Let  $f(x, \mu)$  be any unimodal map that undergoes a period-doubling route to chaos. Suppose that the variables are defined such that the period-2 cycle is born at  $x = 0$  when  $\mu = 0$ . Then for both  $x$  and  $\mu$  close to 0, the map is approximated by

$$x_{n+1} = -(1 + \mu)x_n + ax_n^2 + \dots,$$

since the eigenvalue is  $-1$  at the bifurcation. (We are going to neglect all higher order terms in  $x$  and  $\mu$ ; that's why our results will be only approximate.) Without loss of generality we can set  $a = 1$  by rescaling  $x \rightarrow x/a$ . So locally our map has the normal form

$$x_{n+1} = -(1 + \mu)x_n + x_n^2 + \dots \tag{3}$$

Here's the idea: for  $\mu > 0$ , there exist period-2 points, say  $p$  and  $q$ . As  $\mu$  increases,  $p$  and  $q$  themselves will eventually period-double. When this happens, the dynamics of  $f^2$  near  $p$  will necessarily be approximated by a map with the same algebraic form as (3), since all maps have this form near a period-doubling bifurcation. Our strategy is to calculate the map governing the dynamics of  $f^2$  near  $p$ , and renormalize it to look like (3). This defines a renormalization iteration, which in turn leads to a prediction of  $\alpha$  and  $\delta$ .

First, we find  $p$  and  $q$ . By definition of period-2,  $p$  is mapped to  $q$  and  $q$  to  $p$ . Hence (3) yields

$$p = -(1 + \mu)q + q^2, \quad q = -(1 + \mu)p + p^2.$$

By subtracting one of these equations from the other, and factoring out  $p - q$ , we find that  $p + q = \mu$ . Then multiplying the equations together and simplifying yields  $pq = -\mu$ . Hence

$$p = \frac{\mu + \sqrt{\mu^2 + 4\mu}}{2}, \quad q = \frac{\mu - \sqrt{\mu^2 + 4\mu}}{2}.$$

Now shift the origin to  $p$  and look at the local dynamics. Let

$$f(x) = -(1 + \mu)x + x^2.$$

Then  $p$  is a fixed point of  $f^2$ . Expand  $p + \eta_{n+1} = f^2(p + \eta_n)$  in powers of the small deviation  $\eta_n$ . After some algebra (Exercise 10.7.10) and neglecting higher order terms as usual, we get

$$\eta_{n+1} = (1 - 4\mu - \mu^2)\eta_n + C\eta_n^2 + \dots \quad (4)$$

where

$$C = 4\mu + \mu^2 - 3\sqrt{\mu^2 + 4\mu}. \quad (5)$$

As promised, the  $\eta$ -map (4) has the same algebraic form as the original map (3)! We can renormalize (4) into (3) by rescaling  $\eta$  and by defining a new  $\mu$ . (Note: The need for *both* of these steps was anticipated in the abstract version of renormalization discussed earlier. We have to rescale the state variable  $\eta$  *and* shift the bifurcation parameter  $\mu$ .)

To rescale  $\eta$ , let  $\tilde{x}_n = C\eta_n$ . Then (4) becomes

$$\tilde{x}_{n+1} = (1 - 4\mu - \mu^2)\tilde{x}_n + \tilde{x}_n^2 + \dots \quad (6)$$

This matches (3) almost perfectly. All that remains is to define a new parameter  $\tilde{\mu}$  by  $-(1 + \tilde{\mu}) = (1 - 4\mu - \mu^2)$ . Then (6) achieves the desired form

$$\tilde{x}_{n+1} = -(1 + \tilde{\mu})\tilde{x}_n + \tilde{x}_n^2 + \dots \quad (7)$$

where the renormalized parameter  $\tilde{\mu}$  is given by

$$\tilde{\mu} = \mu^2 + 4\mu - 2. \quad (8)$$

When  $\tilde{\mu} = 0$  the renormalized map (7) undergoes a flip bifurcation. Equivalently, the 2-cycle for the original map loses stability and creates a 4-cycle. This brings us to the end of the first period-doubling.

### EXAMPLE 10.7.2:

Using (8), calculate the value of  $\mu$  at which the original map (3) gives birth to a period-4 cycle. Compare your result to the value  $r_2 = 1 + \sqrt{6}$  found for the logistic map in Example 10.3.3.

*Solution:* The period-4 solution is born when  $\tilde{\mu} = \mu^2 + 4\mu - 2 = 0$ . Solving this quadratic equation yields  $\mu = -2 + \sqrt{6}$ . (The other solution is negative and is not relevant.) Now recall that the origin of  $\mu$  was defined such that  $\mu = 0$  at the birth of period-2, which occurs at  $r = 3$  for the logistic map. Hence  $r_2 = 3 + (-2 + \sqrt{6}) = 1 + \sqrt{6}$ , which recovers the result obtained in Example 10.3.3. ■

Because (7) has the same form as the original map, we can do the same analysis all over again, now regarding (7) as the fundamental map. In other words, we can renormalize *ad infinitum!* This allows us to bootstrap our way to the onset of chaos, using only the **renormalization transformation** (8).

Let  $\mu_k$  denote the parameter value at which the original map (3) gives birth to a  $2^k$ -cycle. By definition of  $\mu$ , we have  $\mu_1 = 0$ ; by Example 10.7.2,  $\mu_2 = -2 + \sqrt{6} \approx 0.449$ . In general, the  $\mu_k$  satisfy

$$\mu_{k-1} = \mu_k^2 + 4\mu_k - 2. \quad (9)$$

At first it looks like we have the subscripts backwards, but think about it, using Example 10.7.2 as a guide. To obtain  $\mu_2$ , we set  $\tilde{\mu} = 0$  ( $= \mu_1$ ) in (8) and then solved for  $\mu$ . Similarly, to obtain  $\mu_k$ , we set  $\tilde{\mu} = \mu_{k-1}$  in (8) and then solve for  $\mu$ .

To convert (9) into a forward iteration, solve for  $\mu_k$  in terms of  $\mu_{k-1}$ :

$$\mu_k = -2\sqrt{6 + \mu_{k-1}}. \quad (10)$$

Exercise 10.7.11 asks you to give a cobweb analysis of (10), starting from the initial condition  $\mu_1 = 0$ . You'll find that  $\mu_k \rightarrow \mu^*$ , where  $\mu^* > 0$  is a stable fixed point corresponding to the onset of chaos.

### EXAMPLE 10.7.3:

Find  $\mu^*$ .

*Solution:* It is slightly easier to work with (9). The fixed point satisfies  $\mu^* = (\mu^*)^2 + 4\mu^* - 2$ , and is given by

$$\mu^* = \frac{1}{2}(-3 + \sqrt{17}) \approx 0.56. \quad (II)$$

Incidentally, this gives a remarkably accurate prediction of  $r_\infty$  for the logistic map. Recall that  $\mu = 0$  corresponds to the birth of period-2, which occurs at  $r = 3$  for the logistic map. Thus  $\mu^*$  corresponds to  $r_\infty \approx 3.56$  whereas the actual numerical result is  $r_\infty \approx 3.57$ ! ■

Finally we get to see how  $\delta$  and  $\alpha$  make their entry. For  $k \gg 1$ , the  $\mu_k$  should converge geometrically to  $\mu^*$  at a rate given by the universal constant  $\delta$ . Hence  $\delta \approx (\mu_{k-1} - \mu^*)/(\mu_k - \mu^*)$ . As  $k \rightarrow \infty$ , this ratio tends to 0/0 and therefore may be evaluated by L'Hôpital's rule. The result is

$$\begin{aligned}\delta &\approx \left. \frac{d\mu_{k-1}}{d\mu_k} \right|_{\mu=\mu^*} \\ &= 2\mu^* + 4\end{aligned}$$

where we have used (9) in calculating the derivative. Finally, we substitute for  $\mu^*$  using (11) and obtain

$$\delta \approx 1 + \sqrt{17} \approx 5.12.$$

This estimate is about 10 percent larger than the true  $\delta \approx 4.67$ , which is not bad considering our approximations.

To find the approximate  $\alpha$ , note that we used  $C$  as a rescaling parameter when we defined  $\tilde{x}_n = C\eta_n$ . Hence  $C$  plays the role of  $\alpha$ . Substitution of  $\mu^*$  into (5) yields

$$C = \frac{1 + \sqrt{17}}{2} - 3 \left[ \frac{1 + \sqrt{17}}{2} \right]^{1/2} \approx -2.24,$$

which is also within 10 percent of the actual value  $\alpha \approx -2.50$ .

## EXERCISES FOR CHAPTER 10

**Note:** Many of these exercises ask you to use a computer. Feel free to write your own programs, or to use commercially available software.

### 10.1 Fixed Points and Cobwebs

(Calculator experiments) Use a pocket calculator to explore the following maps. Start with some number and then keep pressing the appropriate function key; what happens? Then try a different number—is the eventual pattern the same?

If possible, explain your results mathematically, using a cobweb or some other argument.

**10.1.1**  $x_{n+1} = \sqrt{x_n}$

**10.1.2**  $x_{n+1} = x_n^3$

**10.1.3**  $x_{n+1} = \exp x_n$

**10.1.4**  $x_{n+1} = \ln x_n$

**10.1.5**  $x_{n+1} = \cot x_n$

**10.1.6**  $x_{n+1} = \tan x_n$

**10.1.7**  $x_{n+1} = \sinh x_n$

**10.1.8**  $x_{n+1} = \tanh x_n$

**10.1.9** Analyze the map  $x_{n+1} = 2x_n/(1 + x_n)$  for both positive and negative  $x_n$ .

**10.1.10** Show that the map  $x_{n+1} = 1 + \frac{1}{2}\sin x_n$  has a unique fixed point. Is it stable?

**10.1.11** (Cubic map) Consider the map  $x_{n+1} = 3x_n - x_n^3$ .

a) Find all the fixed points and classify their stability.

b) Draw a cobweb starting at  $x_0 = 1.9$ .

c) Draw a cobweb starting at  $x_0 = 2.1$ .

d) Try to explain the dramatic difference between the orbits found in parts (b) and

(c). For instance, can you prove that the orbit in (b) will remain bounded for all  $n$ ? Or that  $|x_n| \rightarrow \infty$  in (c)?

**10.1.12** (Newton's method) Suppose you want to find the roots of an equation  $g(x) = 0$ . Then **Newton's method** says you should consider the map  $x_{n+1} = f(x_n)$ , where

$$f(x_n) = x_n - \frac{g(x_n)}{g'(x_n)}.$$

a) To calibrate the method, write down the “Newton map”  $x_{n+1} = f(x_n)$  for the equation  $g(x) = x^2 - 4 = 0$ .

b) Show that the Newton map has fixed points at  $x^* = \pm 2$ .

c) Show that these fixed points are *superstable*.

d) Iterate the map numerically, starting from  $x_0 = 1$ . Notice the extremely rapid convergence to the right answer!

**10.1.13** (Newton's method and superstability) Generalize Exercise 10.1.12 as follows. Show that (under appropriate circumstances, to be stated) the roots of an equation  $g(x) = 0$  *always* correspond to superstable fixed points of the Newton map  $x_{n+1} = f(x_n)$ , where  $f(x_n) = x_n - g(x_n)/g'(x_n)$ . (This explains why Newton's method converges so fast—if it converges at all.)

**10.1.14** Prove that  $x^* = 0$  is a globally stable fixed point for the map  $x_{n+1} = -\sin x_n$ . (Hint: Draw the line  $x_{n+1} = -x_n$  on your cobweb diagram, in addition to the usual line  $x_{n+1} = x_n$ .)

## 10.2 Logistic Map: Numerics

**10.2.1** Consider the logistic map for all real  $x$  and for any  $r > 1$ .

- Show that if  $x_n > 1$  for some  $n$ , then subsequent iterations diverge toward  $-\infty$ . (For the application to population biology, this means the population goes extinct.)
- Given the result of part (a), explain why it is sensible to restrict  $r$  and  $x$  to the intervals  $r \in [0,4]$  and  $x \in [0,1]$ .

**10.2.2** Use a cobweb to show that  $x^* = 0$  is globally stable for  $0 \leq r \leq 1$  in the logistic map.

**10.2.3** Compute the orbit diagram for the logistic map.

Plot the orbit diagram for each of the following maps. Be sure to use a large enough range for both  $r$  and  $x$  to include the main features of interest. Also, try different initial conditions, just in case it matters.

**10.2.4**  $x_{n+1} = x_n e^{-r(1-x_n)}$  (Standard period-doubling route to chaos)

**10.2.5**  $x_{n+1} = e^{-rx_n}$  (One period-doubling bifurcation and the show is over)

**10.2.6**  $x_{n+1} = r \cos x_n$  (Period-doubling and chaos galore)

**10.2.7**  $x_{n+1} = r \tan x_n$  (Nasty mess)

**10.2.8**  $x_{n+1} = rx_n - x_n^3$  (Attractors sometimes come in symmetric pairs)

## 10.3 Logistic Map: Analysis

**10.3.1** (Superstable fixed point) Find the value of  $r$  at which the logistic map has a superstable fixed point.

**10.3.2** (Superstable 2-cycle) Let  $p$  and  $q$  be points in a 2-cycle for the logistic map.

- Show that if the cycle is *superstable*, then either  $p = \frac{1}{2}$  or  $q = \frac{1}{2}$ . (In other words, the point where the map takes on its maximum must be one of the points in the 2-cycle.)
- Find the value of  $r$  at which the logistic map has a superstable 2-cycle.

**10.3.3** Analyze the long-term behavior of the map  $x_{n+1} = rx_n/(1+x_n^2)$ , where  $r > 0$ . Find and classify all fixed points as a function of  $r$ . Can there be periodic solutions? Chaos?

**10.3.4** (Quadratic map) Consider the *quadratic map*  $x_{n+1} = x_n^2 + c$ .

- Find and classify all the fixed points as a function of  $c$ .
- Find the values of  $c$  at which the fixed points bifurcate, and classify those bifurcations.

- c) For which values of  $c$  is there a stable 2-cycle? When is it superstable?  
d) Plot a partial bifurcation diagram for the map. Indicate the fixed points, the 2-cycles, and their stability.

**10.3.5** (Conjugacy) Show that the logistic map  $x_{n+1} = rx_n(1 - x_n)$  can be transformed into the quadratic map  $y_{n+1} = y_n^2 + c$  by a linear change of variables,  $x_n = ay_n + b$ , where  $a, b$  are to be determined.

(One says that the logistic and quadratic maps are “conjugate.” More generally, a *conjugacy* is a change of variables that transforms one map into another. If two maps are conjugate, they are equivalent as far as their dynamics are concerned; you just have to translate from one set of variables to the other. Strictly speaking, the transformation should be a homeomorphism, so that all topological features are preserved.)

**10.3.6** (Cubic map) Consider the cubic map  $x_{n+1} = f(x_n)$ , where  $f(x_n) = rx_n - x_n^3$ .

- Find the fixed points. For which values of  $r$  do they exist? For which values are they stable?
- To find the 2-cycles of the map, suppose that  $f(p) = q$  and  $f(q) = p$ . Show that  $p, q$  are roots of the equation  $x(x^2 - r + 1)(x^2 - r - 1)(x^4 - rx^2 + 1) = 0$  and use this to find all the 2-cycles.
- Determine the stability of the 2-cycles as a function of  $r$ .
- Plot a partial bifurcation diagram, based on the information obtained.

**10.3.7** (A chaotic map that can be analyzed completely) Consider the *decimal shift map* on the unit interval given by

$$x_{n+1} = 10x_n \pmod{1}.$$

As usual, “mod 1” means that we look only at the noninteger part of  $x$ . For example,  $2.63 \pmod{1} = 0.63$ .

- Draw the graph of the map.
- Find all the fixed points. (Hint: Write  $x_n$  in decimal form.)
- Show that the map has periodic points of all periods, but that all of them are unstable. (For the first part, it suffices to give an explicit example of a period- $p$  point, for each integer  $p > 1$ .)
- Show that the map has infinitely many aperiodic orbits.
- By considering the rate of separation between two nearby orbits, show that the map has sensitive dependence on initial conditions.

**10.3.8** (Dense orbit for the decimal shift map) Consider a map of the unit interval into itself. An orbit  $\{x_n\}$  is said to be “dense” if it eventually gets arbitrarily close to every point in the interval. Such an orbit has to hop around rather crazily! More precisely, given any  $\varepsilon > 0$  and any point  $p \in [0,1]$ , the orbit  $\{x_n\}$  is *dense* if there is some finite  $n$  such that  $|x_n - p| < \varepsilon$ .

Explicitly construct a dense orbit for the decimal shift map  $x_{n+1} = 10x_n \pmod{1}$ .

**10.3.9** (Binary shift map) Show that the **binary shift map**  $x_{n+1} = 2x_n \pmod{1}$  has sensitive dependence on initial conditions, infinitely many periodic and aperiodic orbits, and a dense orbit. (Hint: Redo Exercises 10.3.7 and 10.3.8, but write  $x_n$  as a binary number, not a decimal.)

**10.3.10** (Exact solutions for the logistic map with  $r = 4$ ) The previous exercise shows that the orbits of the binary shift map can be wild. Now we are going to see that this same wildness occurs in the logistic map when  $r = 4$ .

a) Let  $\{\theta_n\}$  be an orbit of the binary shift map  $\theta_{n+1} = 2\theta_n \pmod{1}$ , and define a new sequence  $\{x_n\}$  by  $x_n = \sin^2(\pi\theta_n)$ . Show that  $x_{n+1} = 4x_n(1 - x_n)$ , no matter what  $\theta_0$  we started with. Hence any such orbit is an exact solution of the logistic map with  $r = 4$ !

b) Graph the time series  $x_n$  vs.  $n$ , for various choices of  $\theta_0$ .

**10.3.11** (Subcritical flip) Let  $x_{n+1} = f(x_n)$ , where  $f(x) = -(1+r)x - x^2 - 2x^3$ .

a) Classify the linear stability of the fixed point  $x^* = 0$ .

b) Show that a flip bifurcation occurs at  $x^* = 0$  when  $r = 0$ .

c) By considering the first few terms in the Taylor series for  $f^2(x)$  or otherwise, show that there is an *unstable* 2-cycle for  $r < 0$ , and that this cycle coalesces with  $x^* = 0$  as  $r \rightarrow 0$  from below.

d) What is the long-term behavior of orbits that start near  $x^* = 0$ , both for  $r < 0$  and  $r > 0$ ?

**10.3.12** (Numerics of superstable cycles) Let  $R_n$  denote the value of  $r$  at which the logistic map has a superstable cycle of period  $2^n$ .

a) Write an implicit but exact formula for  $R_n$  in terms of the point  $x = \frac{1}{2}$  and the function  $f(x, r) = rx(1 - x)$ .

b) Using a computer and the result of part (a), find  $R_2, R_3, \dots, R_7$  to five significant figures.

c) Evaluate  $\frac{R_6 - R_5}{R_7 - R_6}$ .

**10.3.13** (Tantalizing patterns) The orbit diagram of the logistic map (Figure 10.2.7) exhibits some striking features that are rarely discussed in books.

a) There are several smooth, dark tracks of points running through the chaotic part of the diagram. What are these curves? (Hint: Think about  $f(x_m, r)$ , where  $x_m = \frac{1}{2}$  is the point at which  $f$  is maximized.)

b) Can you find the exact value of  $r$  at the corner of the “big wedge”? (Hint: Several of the dark tracks in part (b) intersect at this corner.)

## 10.4 Periodic Windows

**10.4.1** (Exponential map) Consider the map  $x_{n+1} = r \exp x_n$  for  $r > 0$ .

a) Analyze the map by drawing a cobweb.

- b) Show that a tangent bifurcation occurs at  $r = 1/e$ .  
 c) Sketch the time series  $x_n$  vs.  $n$  for  $r$  just above and just below  $r = 1/e$ .

**10.4.2** Analyze the map  $x_{n+1} = rx_n^2/(1 + x_n^2)$ . Find and classify all the bifurcations and draw the bifurcation diagram. Can this system exhibit intermittency?

**10.4.3** (A superstable 3-cycle) The map  $x_{n+1} = 1 - rx_n^2$  has a superstable 3-cycle at a certain value of  $r$ . Find a cubic equation for this  $r$ .

**10.4.4** Approximate the value of  $r$  at which the logistic map has a superstable 3-cycle. Please give a numerical approximation that is accurate to at least four places after the decimal point.

**10.4.5** (Band merging and crisis) Show numerically that the period-doubling bifurcations of the 3-cycle for the logistic map accumulate near  $r = 3.8495\ldots$ , to form three small chaotic bands. Show that these chaotic bands merge near  $r = 3.857\ldots$  to form a much larger attractor that nearly fills an interval.

This discontinuous jump in the size of an attractor is an example of a *crisis* (Grebogi, Ott, and Yorke 1983a).

**10.4.6** (A superstable cycle) Consider the logistic map with  $r = 3.7389149$ . Plot the cobweb diagram, starting from  $x_0 = \frac{1}{2}$  (the maximum of the map). You should find a superstable cycle. What is its period?

**10.4.7** (Iteration patterns) Superstable cycles for the logistic map can be characterized by a string of *R*'s and *L*'s, as follows. By convention, we start the cycle at  $x_0 = \frac{1}{2}$ . Then if the  $n$ th iterate  $x_n$  lies to the right of  $x_0 = \frac{1}{2}$ , the  $n$ th letter in the string is an *R*; otherwise it's an *L*. (No letter is used if  $x_n = \frac{1}{2}$ , since the superstable cycle is then complete.) The string is called the *symbol sequence* or *iteration pattern* for the superstable cycle (Metropolis et al. 1973).

a) Show that for the logistic map with  $r > 1 + \sqrt{5}$ , the first two letters are always *RL*.

b) What is the iteration pattern for the orbit you found in Exercise 10.4.6?

**10.4.8** (Intermittency in the Lorenz equations) Solve the Lorenz equations numerically for  $\sigma = 10$ ,  $b = \frac{8}{3}$ , and  $r$  near 166.

- a) Show that if  $r = 166$ , all trajectories are attracted to a stable limit cycle. Plot both the  $xz$  projection of the cycle, and the time series  $x(t)$ .  
 b) Show that if  $r = 166.2$ , the trajectory looks like the old limit cycle for much of the time, but occasionally it is interrupted by chaotic bursts. This is the signature of intermittency.  
 c) Show that as  $r$  increases, the bursts become more frequent and last longer.

**10.4.9** (Period-doubling in the Lorenz equations) Solve the Lorenz equations numerically for  $\sigma = 10$ ,  $b = \frac{8}{3}$ , and  $r = 148.5$ . You should find a stable limit cycle. Then repeat the experiment for  $r = 147.5$  to see a period-doubled version of this

cycle. (When plotting your results, discard the initial transient, and use the  $xy$  projections of the attractors.)

**10.4.10** (The birth of period 3) This is a hard exercise. The goal is to show that the period-3 cycle of the logistic map is born in a tangent bifurcation at  $r = 1 + \sqrt{8} = 3.8284\dots$ . Here are a few vague hints. There are four unknowns: the three period-3 points  $a, b, c$  and the bifurcation value  $r$ . There are also four equations:  $f(a) = b$ ,  $f(b) = c$ ,  $f(c) = a$ , and the tangent bifurcation condition. Try to eliminate  $a, b, c$  (which we don't care about anyway) and get an equation for  $r$  alone. It may help to shift coordinates so that the map has its maximum at  $x = 0$  rather than  $x = \frac{1}{2}$ . Also, you may want to change variables again to symmetric polynomials involving sums of products of  $a, b, c$ . See Saha and Strogatz (1995) for one solution, probably not the most elegant one!

**10.4.11** (Repeated exponentiation) Let  $a > 0$  be an arbitrary positive real number, and consider the following sequence:

$$x_1 = a$$

$$x_2 = a^a$$

$$x_3 = a^{(a^a)}$$

and so on, where the general term is  $x_{n+1} = a^{x_n}$ . Analyze the long-term behavior of the sequence  $\{x_n\}$  as  $n \rightarrow \infty$ , given that  $x_1 = a$ , and then discuss how that long-term behavior depends on  $a$ . For instance, show that for certain values of  $a$ , the terms  $x_n$  tend to some limiting value. How does that limit depend on  $a$ ? For which values of  $a$  is the long-term behavior more complicated? What happens then?

After you finish exploring these questions on your own, you may want to consult Knoebel (1981) and Rippon (1983) for a taste of the extensive history surrounding iterated exponentials, going all the way back to Euler (1777).

## 10.5 Liapunov Exponent

**10.5.1** Calculate the Liapunov exponent for the linear map  $x_{n+1} = rx_n$ .

**10.5.2** Calculate the Liapunov exponent for the decimal shift map  $x_{n+1} = 10x_n \pmod{1}$ .

**10.5.3** Analyze the dynamics of the tent map for  $r \leq 1$ .

**10.5.4** (No windows for the tent map) Prove that, in contrast to the logistic map, the tent map does *not* have periodic windows interspersed with chaos.

**10.5.5** Plot the orbit diagram for the tent map.

**10.5.6** Using a computer, compute and plot the Liapunov exponent as a function of  $r$  for the sine map  $x_{n+1} = r \sin \pi x_n$ , for  $0 \leq x_n \leq 1$  and  $0 \leq r \leq 1$ .

**10.5.7** The graph in Figure 10.5.2 suggests that  $\lambda = 0$  at each period-doubling bifurcation value  $r_n$ . Show analytically that this is correct.

## 10.6 Universality and Experiments

The first two exercises deal with the sine map  $x_{n+1} = r \sin \pi x_n$ , where  $0 < r \leq 1$  and  $x \in [0,1]$ . The goal is to learn about some of the practical problems that come up when one tries to estimate  $\delta$  numerically.

### 10.6.1 (Naive approach)

- At each of 200 equally spaced  $r$  values, plot  $x_{700}$  through  $x_{1000}$  vertically above  $r$ , starting from some random initial condition  $x_0$ . Check your orbit diagram against Figure 10.6.2 to be sure your program is working.
- Now go to finer resolution near the period-doubling bifurcations, and estimate  $r_n$ , for  $n = 1, 2, \dots, 6$ . Try to achieve five significant figures of accuracy.
- Use the numbers from (b) to estimate the Feigenbaum ratio  $\frac{r_n - r_{n-1}}{r_{n+1} - r_n}$ .

(Note: To get accurate estimates in part (b), you need to be clever, or careful, or both. As you probably found, a straightforward approach is hampered by “critical slowing down”—the convergence to a cycle becomes unbearably slow when that cycle is on the verge of period-doubling. This makes it hard to decide precisely where the bifurcation occurs. To achieve the desired accuracy, you may have to use double precision arithmetic, and about  $10^4$  iterates. But maybe you can find a shortcut by reformulating the problem.)

**10.6.2** (Superstable cycles to the rescue) The “critical slowing down” encountered in the previous problem is avoided if we compute  $R_n$  instead of  $r_n$ . Here  $R_n$  denotes the value of  $r$  at which the sine map has a superstable cycle of period  $2^n$ .

- Explain why it should be possible to compute  $R_n$  more easily and accurately than  $r_n$ .
- Compute the first six  $R_n$ ’s and use them to estimate  $\delta$ .

If you’re interested in knowing the *best* way to compute  $\delta$ , see Briggs (1991) for the state of the art.

**10.6.3** (Qualitative universality of patterns) The U-sequence dictates the ordering of the windows, but it actually says more: it dictates the *iteration pattern* within each window. (See Exercise 10.4.7 for the definition of iteration patterns.) For instance, consider the large period-6 window for the logistic and sine maps, visible in Figure 10.6.2.

- For both maps, plot the cobweb for the corresponding superstable 6-cycle, given that it occurs at  $r = 3.6275575$  for the logistic map and  $r = 0.8811406$  for the sine map. (This cycle acts as a representative for the whole window.)
- Find the iteration pattern for both cycles, and confirm that they match.

**10.6.4** (Period 4) Consider the iteration patterns of all possible period-4 orbits for the logistic map, or any other unimodal map governed by the U-sequence.

- Show that only two patterns are possible for period-4 orbits: *RLL* and *RLR*.
- Show that the period-4 orbit with pattern *RLL* always occurs after *RLR*, i.e., at a larger value of  $r$ .

**10.6.5** (Unfamiliar later cycles) The final superstable cycles of periods 5, 6, 4, 6, 5, 6 in the logistic map occur at approximately the following values of  $r$ : 3.9057065, 3.9375364, 3.9602701, 3.9777664, 3.9902670, 3.9975831 (Metropolis et al. 1973). Notice that they're all near the end of the orbit diagram. They have tiny windows around them and tend to be overlooked.

- Plot the cobwebs for these cycles.
- Did you find it hard to obtain the cycles of periods 5 and 6? If so, can you explain why this trouble occurred?

**10.6.6** (A trick for locating superstable cycles) Hao and Zheng (1989) give an amusing algorithm for finding a superstable cycle with a specified iteration pattern. The idea works for any unimodal map, but for convenience, consider the map  $x_{n+1} = r - x_n^2$ , for  $0 \leq r \leq 2$ . Define two functions  $R(y) = \sqrt{r - y}$ ,  $L(y) = -\sqrt{r - y}$ . These are the right and left branches of the inverse map.

- For instance, suppose we want to find the  $r$  corresponding to the superstable 5-cycle with pattern *RLLR*. Then Hao and Zheng show that this amounts to solving the equation  $r = RLLR(0)$ . Show that when this equation is written out explicitly, it becomes

$$r = \sqrt{r + \sqrt{r + \sqrt{r - \sqrt{r}}}}.$$

- Solve this equation numerically by iterating the map

$$r_{n+1} = \sqrt{r_n + \sqrt{r_n + \sqrt{r_n - \sqrt{r_n}}}},$$

starting from any reasonable guess, e.g.,  $r_0 = 2$ . Show numerically that  $r_n$  converges rapidly to 1.860782522. . . .

- Verify that the answer to (b) yields a cycle with the desired pattern.

## 10.7 Renormalization

**10.7.1** (Hands on the functional equation) The functional equation  $g(x) = \alpha g^2(x/\alpha)$  arose in our renormalization analysis of period-doubling. Let's

approximate its solution by brute force, assuming that  $g(x)$  is even and has a quadratic maximum at  $x = 0$ .

- Suppose  $g(x) \approx 1 + c_2 x^2$  for small  $x$ . Solve for  $c_2$  and  $\alpha$ . (Neglect  $O(x^4)$  terms.)
- Now assume  $g(x) \approx 1 + c_2 x^2 + c_4 x^4$ , and use Mathematica, Maple, Macsyma (or hand calculation) to solve for  $\alpha, c_2, c_4$ . Compare your approximate results to the “exact” values  $\alpha \approx -2.5029 \dots, c_2 \approx -1.527 \dots, c_4 \approx 0.1048 \dots$

**10.7.2** Given a map  $y_{n+1} = f(y_n)$ , rewrite the map in terms of a rescaled variable  $x_n = \alpha y_n$ . Use this to show that rescaling and inversion converts  $f^2(x, R_1)$  into  $\alpha f^2(x/\alpha, R_1)$ , as claimed in the text.

**10.7.3** Show that if  $g$  is a solution of the functional equation, so is  $\mu g(x/\mu)$ , with the same  $\alpha$ .

**10.7.4** (Wildness of the universal function  $g(x)$ ) Near the origin  $g(x)$  is roughly parabolic, but elsewhere it must be rather wild. In fact, the function  $g(x)$  has infinitely many wiggles as  $x$  ranges over the real line. Verify these statements by demonstrating that  $g(x)$  crosses the lines  $y = \pm x$  infinitely many times. (Hint: Show that if  $x^*$  is a fixed point of  $g(x)$ , then so is  $\alpha x^*$ .)

**10.7.5** (Crudest possible estimate of  $\alpha$ ) Let  $f(x, r) = r - x^2$ .

- Write down explicit expressions for  $f(x, R_0)$  and  $\alpha f^2(x/\alpha, R_1)$ .
- The two functions in (a) are supposed to resemble each other near the origin, if  $\alpha$  is chosen correctly. (That’s the idea behind Figure 10.7.3.) Show the  $O(x^2)$  coefficients of the two functions agree if  $\alpha = -2$ .

**10.7.6** (Improved estimate of  $\alpha$ ) Redo Exercise 10.7.5 to one higher order: Let  $f(x, r) = r - x^2$  again, but now compare  $\alpha f^2(x/\alpha, R_1)$  to  $\alpha^2 f^4(x/\alpha^2, R_2)$  and match the coefficients of the lowest powers of  $x$ . What value of  $\alpha$  is obtained in this way?

**10.7.7** (Quartic maxima) Develop the renormalization theory for functions with a *fourth-degree* maximum, e.g.,  $f(x, r) = r - x^4$ . What approximate value of  $\alpha$  is predicted by the methods of Exercises 10.7.1 and 10.7.5? Estimate the first few terms in the power series for the universal function  $g(x)$ . By numerical experimentation, estimate the new value of  $\delta$  for the quartic case.

See Briggs (1991) for precise values of  $\alpha$  and  $\delta$  for this fourth-degree case, as well as for all other integer degrees between 2 and 12.

**10.7.8** (Renormalization approach to intermittency: algebraic version) Consider the map  $x_{n+1} = f(x_n, r)$ , where  $f(x_n, r) = -r + x - x^2$ . This is the normal form for any map close to a tangent bifurcation.

- Show that the map undergoes a tangent bifurcation at the origin when  $r = 0$ .
- Suppose  $r$  is small and positive. By drawing a cobweb, show that a typical orbit takes many iterations to pass through the bottleneck at the origin.

- c) Let  $N(r)$  denote the typical number of iterations of  $f$  required for an orbit to get through the bottleneck. Our goal is to see how  $N(r)$  scales with  $r$  as  $r \rightarrow 0$ . We use a renormalization idea: Near the origin,  $f^2$  looks like a rescaled version of  $f$ , and hence it too has a bottleneck there. Show that it takes approximately  $\frac{1}{2}N(r)$  iterations for orbits of  $f^2$  to pass through the bottleneck.
- d) Expand  $f^2(x,r)$  and keep only the terms through  $O(x^2)$ . Rescale  $x$  and  $r$  to put this new map into the desired normal form  $F(X,R) \approx -R + X - X^2$ . Show that this renormalization implies the recursive relation

$$\frac{1}{2}N(r) \approx N(4r).$$

- e) Show that the equation in (d) has solutions  $N(r) = ar^b$  and solve for  $b$ .

**10.7.9** (Renormalization approach to intermittency: functional version) Show that if the renormalization procedure in Exercise 10.7.8 is done exactly, we are led to the functional equation

$$g(x) = \alpha g^2(x/\alpha)$$

(just as in the case of period-doubling!) but with new boundary conditions appropriate to the tangent bifurcation:

$$g(0) = 0, \quad g'(0) = 1.$$

Unlike the period-doubling case, this functional equation can be solved *explicitly* (Hirsch et al. 1982).

- a) Verify that a solution is  $\alpha = 2$ ,  $g(x) = x/(1+ax)$ , with  $a$  arbitrary.  
 b) Explain why  $\alpha = 2$  is almost obvious, in retrospect. (Hint: Draw cobwebs for both  $g$  and  $g^2$  for an orbit passing through the bottleneck. Both cobwebs look like staircases; compare the lengths of their steps.)

**10.7.10** Fill in the missing algebraic steps in the concrete renormalization calculation for period-doubling. Let  $f(x) = -(1+\mu)x + x^2$ . Expand  $p + \eta_{n+1} = f^2(p + \eta_n)$  in powers of the small deviation  $\eta_n$ , using the fact that  $p$  is a fixed point of  $f^2$ . Thereby confirm that (10.7.4) and (10.7.5) are correct.

**10.7.11** Give a cobweb analysis of (10.7.10), starting from the initial condition  $\mu_1 = 0$ . Show that  $\mu_k \rightarrow \mu^*$ , where  $\mu^* > 0$  is a stable fixed point corresponding to the onset of chaos.